

Introduction to "Synchrotron Radiation Workshop"



NSLS-II @ BNL



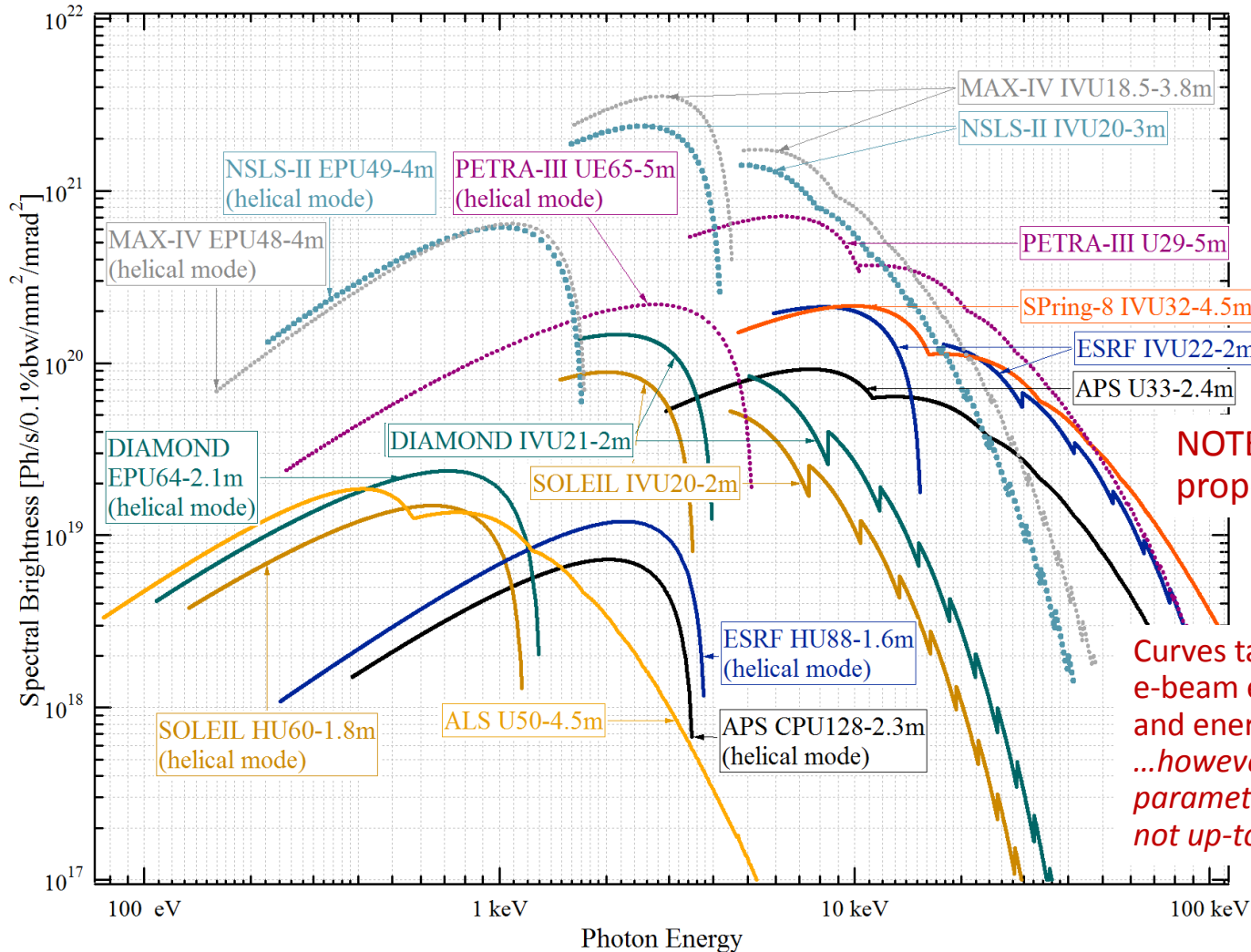
O. Chubar
Photon Sciences Directorate, BNL

Synchrotron Optics Simulations: 3-Codes Tutorial
3 - 5 June 2013, ESRF, France

Outline

1. Light Source Developments Driving the Needed Improvements in X-Ray Optics Simulation and Modeling
2. Some Details of Single-Electron Undulator Radiation
3. Method for Simulation of Emission and Propagation of Partially-Coherent SR
4. Simulation Examples: Beamlines and Experiments
5. Current Status of SRW and Collaborations
6. Summary

Approximate Spectral Brightness of Undulator Sources in 3rd(+) Generation Storage Rings



$\epsilon_x = 0.26 \text{ nm}$

$\epsilon_x = 0.55 \text{ nm}$

$\epsilon_x = 1.0 \text{ nm}$

$\epsilon_x = 3.4 \text{ nm}$

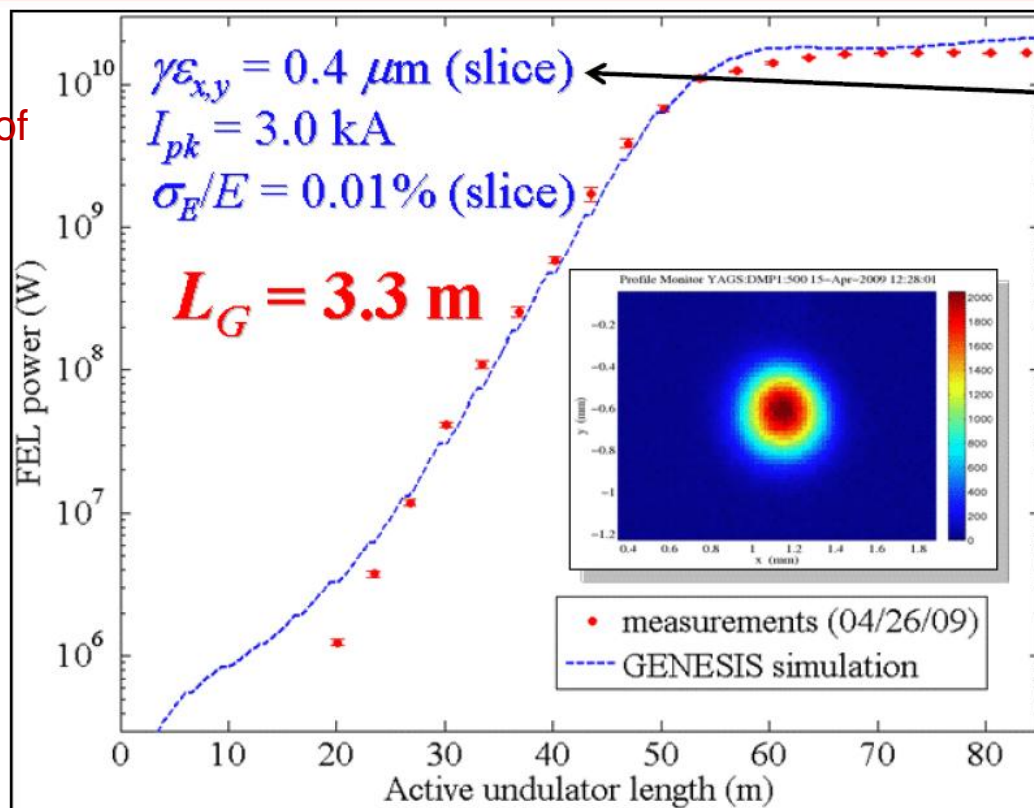
$\epsilon_x = 2.8 \text{ nm}$

NOTE: the "Coherent Flux" is proportional to Brightness:

$$F_{coh} \approx (\lambda/2)^2 B$$

Curves take into account e-beam emittance and energy spread ...however some source parameters may be not up-to-date...

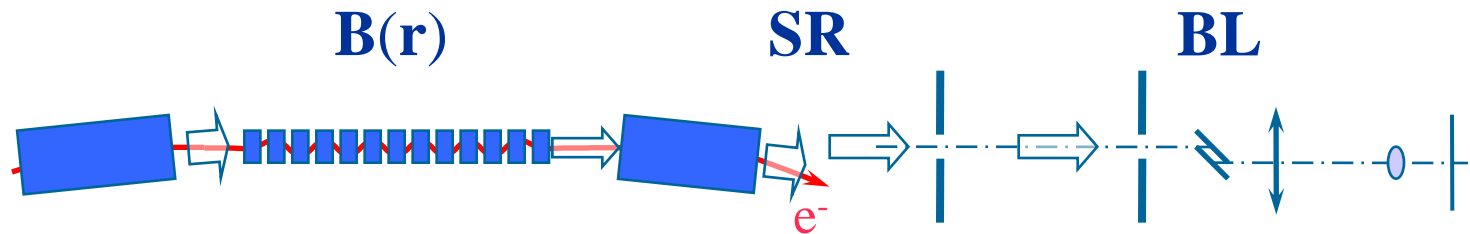
The Turn on of LCLS: First Performance Exceeds Expectation



From presentations of
P. S. Drell (2009)
P. Emma, PAC-2009

- Typical x-ray beam energy $> 1 \text{ mJ}$ or $> 10^{12}$ photons per pulse
- Typical x-ray pulse duration at 300 pC charge $\sim 100 \text{ fs}$ (FWHM).
- X-ray pulse duration at 20 pC charge $< 10 \text{ fs}$
- Saturation at 65 m (anticipated 87 m)

General Motivation: Start To End Simulation



- Computation of **Magnetic Fields** produced by Permanent Magnets, Coils and Iron Blocks and in 3D space, optimized for the design of **Accelerator Magnets, Undulators and Wigglers**
- Fast computation of **Synchrotron Radiation** emitted by relativistic electrons in Magnetic Field of arbitrary configuration
- **SR Wavefront Propagation** (Physical Optics)
- Simulation of some **Experiments** involving **SR**

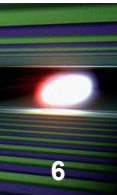
RADIA



SRW

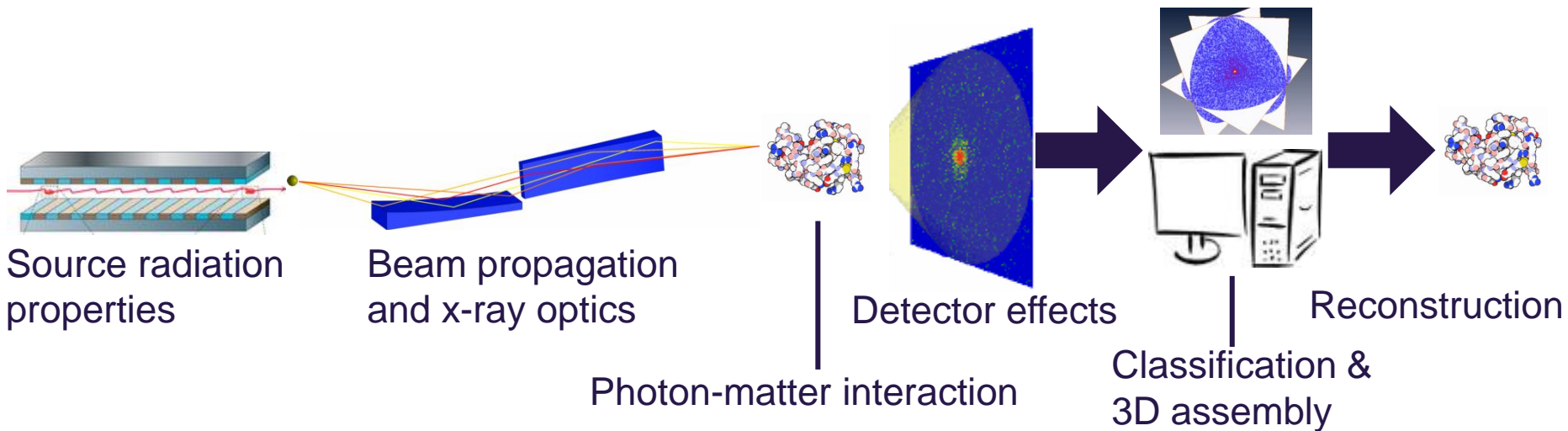
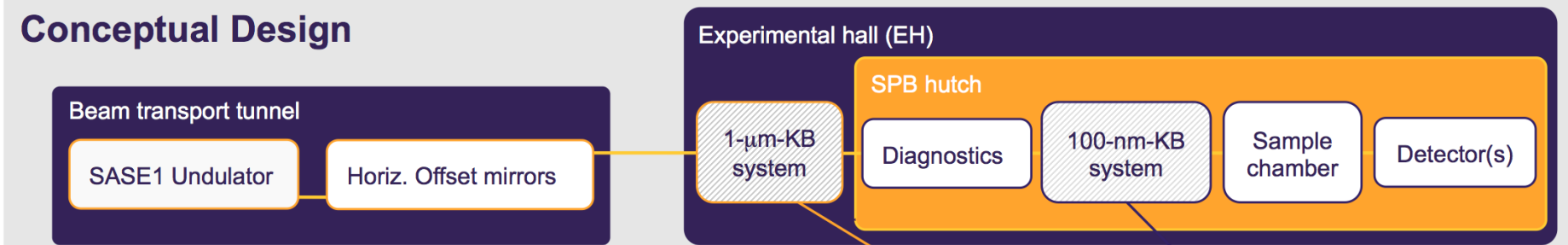
Started at ESRF
thanks to
Pascal Elleaume

Single particle imaging at the SPB instrument of the European XFEL—from start to end II



Courtesy of A. P. Mancuso and L. Samoylova

Conceptual Design



Images: *Nature Photonics* 4, 814–821 (2010), x-ray-optics.de, pdb.org, J. Phys. B: At. Mol. Opt. Phys. 43 (2010) 194016, SPB CDR

Some Computer Codes for Synchrotron Radiation and X-Ray Optics Simulation

• Synchrotron Radiation

Spontaneous

- URGENT (R. Walker, ELETTRA)
- XOP (M.S. del Rio, ESRF, R. Dejus, APS)
- SPECTRA (T. Tanaka, H. Kitamura, SPring-8)
- WAVE (M. Scheer, BESSY)
- B2E (P. Elleaume, ESRF, 1994)
- SRW (O. Chubar, P. Elleaume, ESRF, 1997-...)
- SRCalc (R. Reininger, 2000)

• Geometrical Ray-Tracing

- SHADOW (F. Cerrina, M.S. del Rio)
- RAY (F. Schäfers, BESSY)
- McXtrace (E. Knudsen, A. Prodi, P. Willendrup, K. Lefmann, Univ. Copenhagen)

• Wavefront Propagation

- PHASE (J. Bahrtdt, BESSY)
- SRW (O. Chubar, P. Elleaume, ESRF, 1997-...)
- Code of J. Krzywinski et. al. (SLAC)
- Code of L. Poyneer et. al. (LLNL)

Free

SASE (3D)

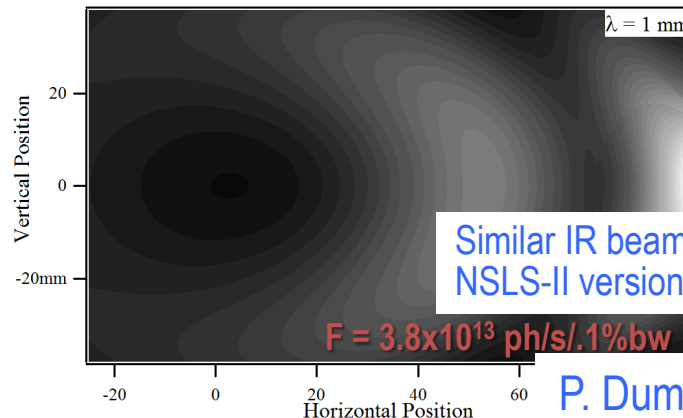
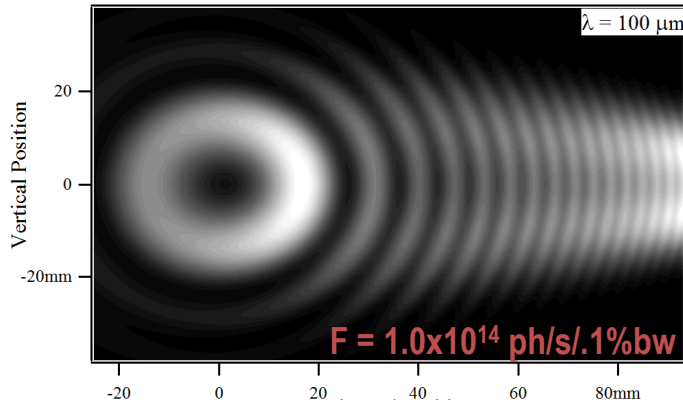
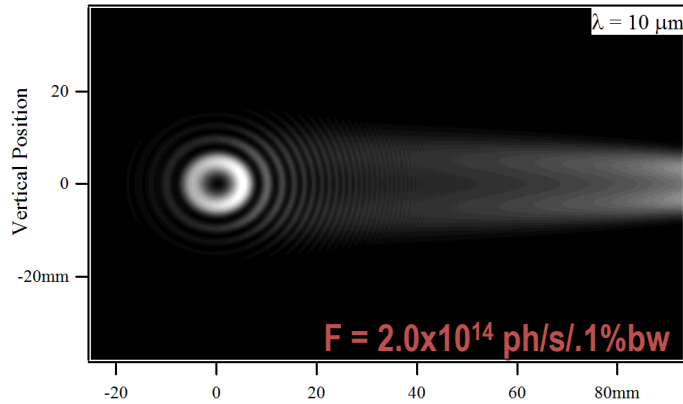
- GENESIS (S. Reiche, DESY/UCLA/PSI, ~1990-...)
- GINGER (W.M. Fawley, LBNL, ~1986-...)
- FAST (M. Yurkov, E. Schneidmiller, DESY, ~1990-...)

Commercial

- ZEMAX (Radiant Zemax)
- GLAD (Applied Optics Research)
- VirtualLab (LightTrans)
- OSLO (Sinclair Optics)
- Microwave Studio (CST)

Commercial codes are expensive, and yet don't have all functions required for SR / X-ray Optics simulations

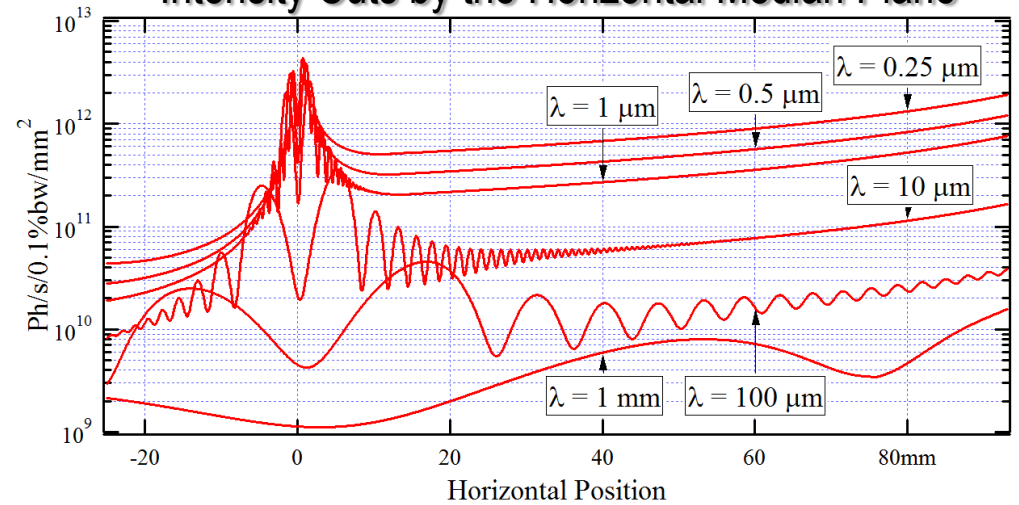
IR SR / ER Intensity Distributions in Transverse Plane at M1 of an Infrared Beamline of NSLS-II



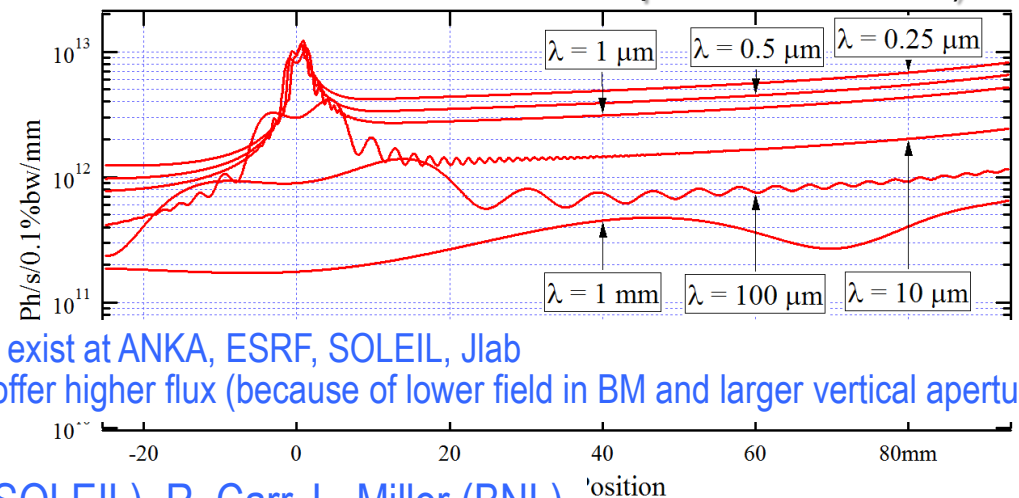
Similar IR beamlines exist at ANKA, ESRF, SOLEIL, Jlab
 NSLS-II version will offer higher flux (because of lower field in BM and larger vertical aperture)

$B = 0.4 \text{ T}$; Collection Aperture: $\sim 50 \text{ mrad (h)} \times 35 \text{ mrad (v)}$

Intensity Cuts by the Horizontal Median Plane



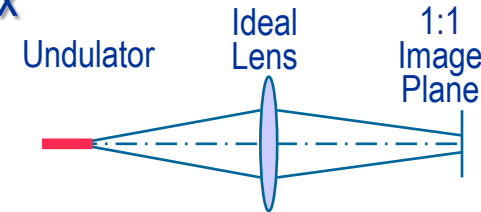
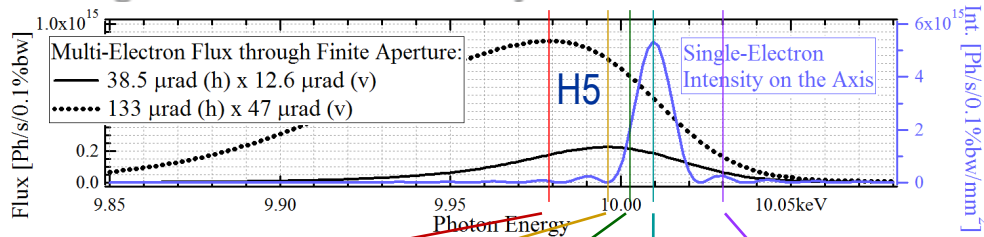
Intensity Profiles (obtained by integration of 2D distributions over vertical position within M1)



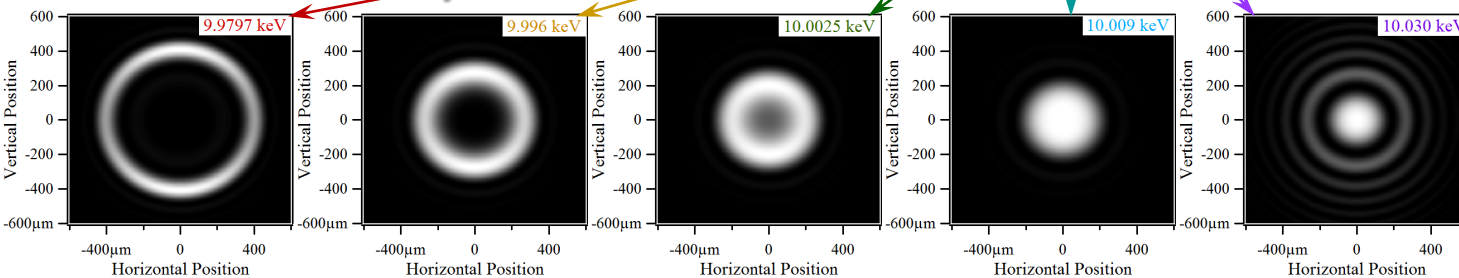
Single-Electron (Fully Transversely-Coherent) UR Intensity Distributions “in Far Field” and “at Source”

UR “Single-Electron” Intensity and “Multi-Electron” Flux

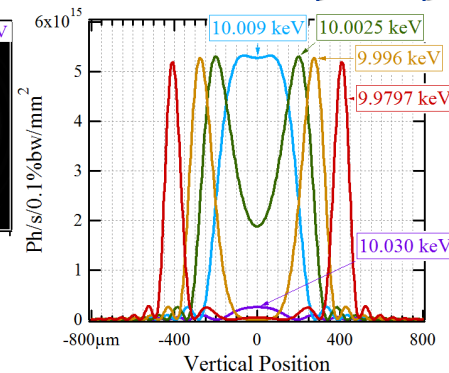
E-Beam Energy: 3 GeV
Current: 0.5 A
Undulator Period: 20 mm



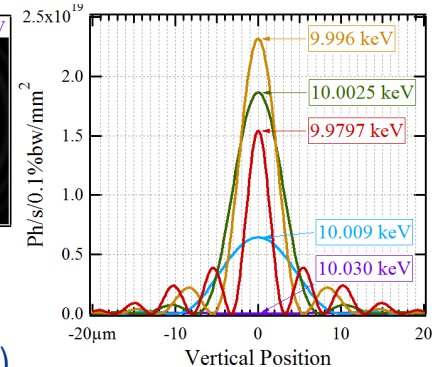
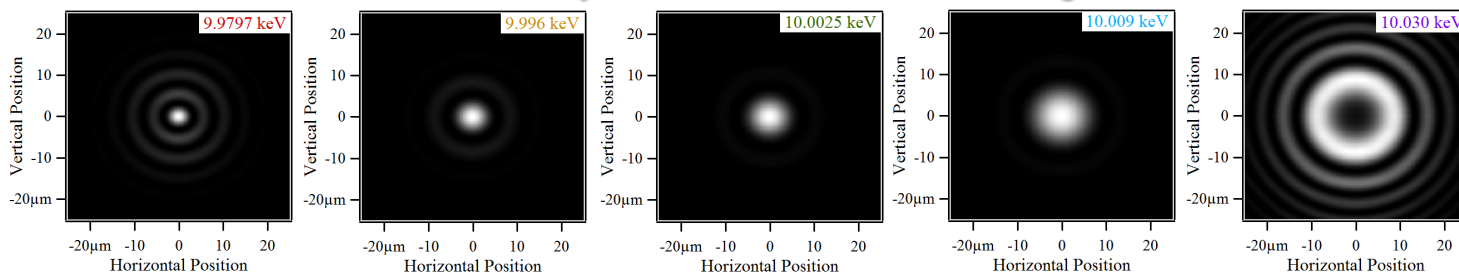
Intensity Distributions at 30 m from Undulator Center



Vertical Cuts (x = 0)



Intensity Distributions in 1:1 Image Plane



“Phase-Space Volume” Estimation for Vertical Plane

(RMS sizes/divergences calculated for the portions of intensity distributions containing 95% of flux)

$$\sigma_y \sigma_y' \approx 7.7 \frac{\lambda}{4\pi}$$

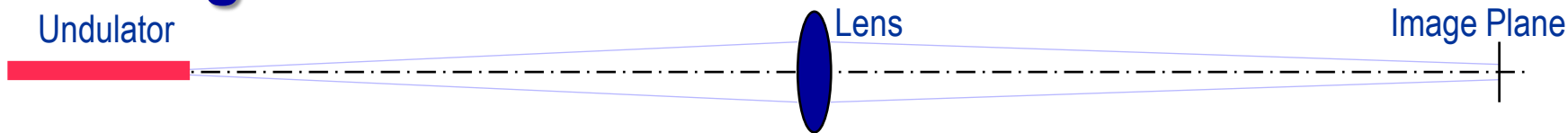
$$3.3 \frac{\lambda}{4\pi}$$

$$1.9 \frac{\lambda}{4\pi}$$

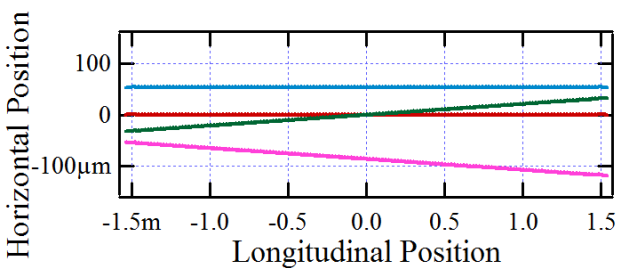
$$1.5 \frac{\lambda}{4\pi}$$

$$9.2 \frac{\lambda}{4\pi}$$

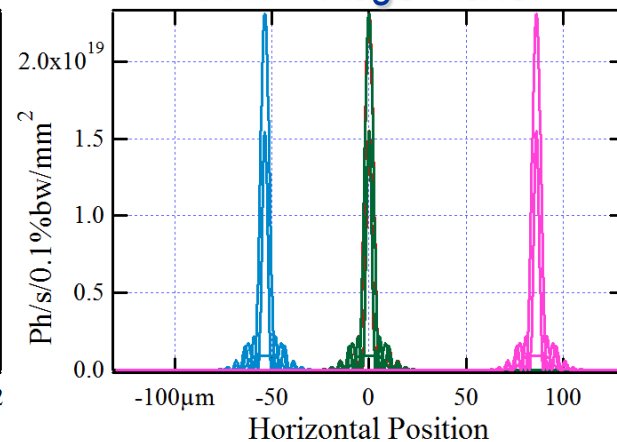
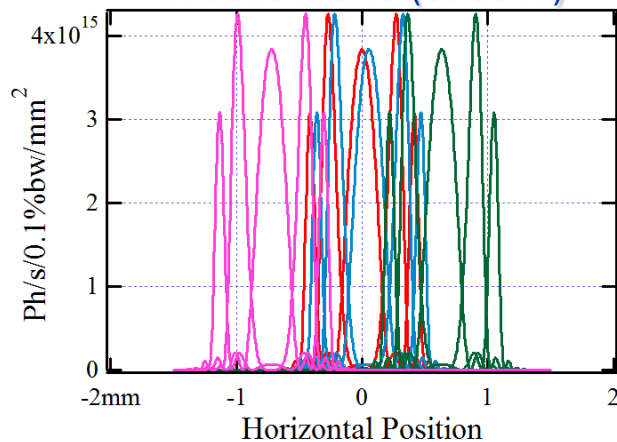
Formation of Intensity Distribution of Partially-Coherent Spontaneous SR after Propagation through a Beamline in a 3rd Generation Source



Electron Trajectories

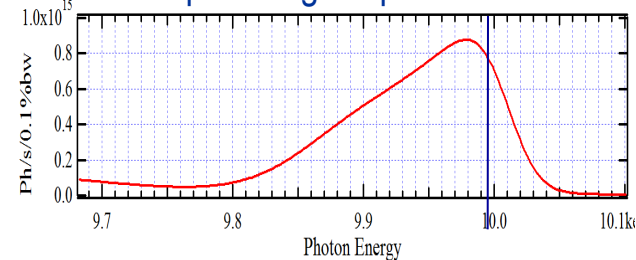


“Single-Electron” Intensity Distributions (Horizontal Cuts) In Lens Plane (at 30 m) In 1:1 Image Plane

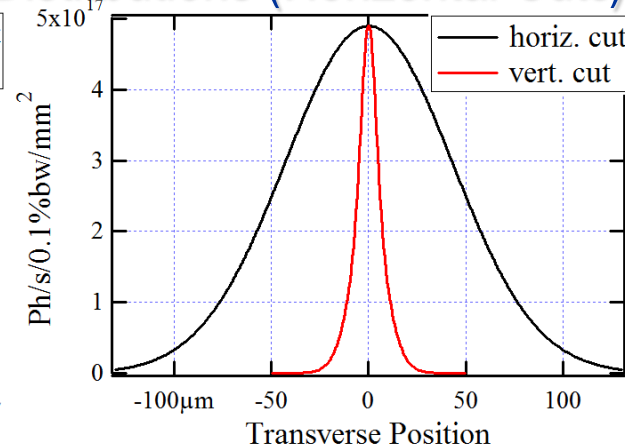
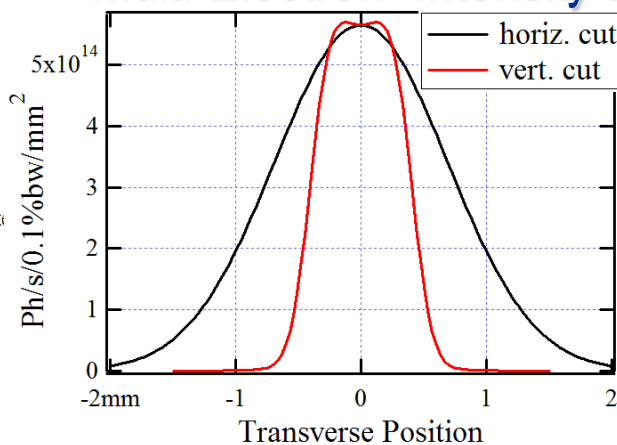


UR Spectrum

through 100 μrad (H) x 50 μrad (V) Ap. at K~1.5 providing H5 peak at ~10 keV



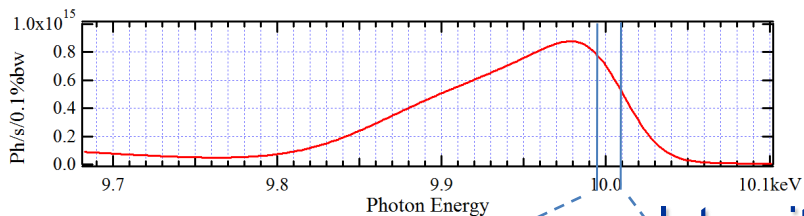
“Multi-Electron” Intensity Distributions (Horizontal Cuts)



Estimation of X-Ray Beam Angular Divergence and Source Size by Wavefront Propagation

IVU20-3m Spectral Flux

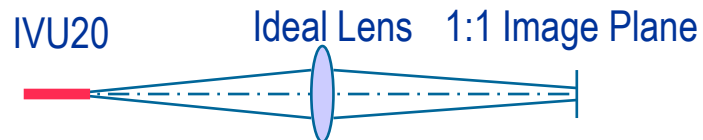
through 100 μrad (H) x 50 μrad (V) Aperture at K~1.5 providing H5 peak at ~10 keV



Electron Beam:

- Hor. Emittance: 0.9 nm
- Vert. Emittance: 8 pm
- Energy Spread: 8.9×10^{-4}
- Current: 0.5 A
- Low-Beta Straight

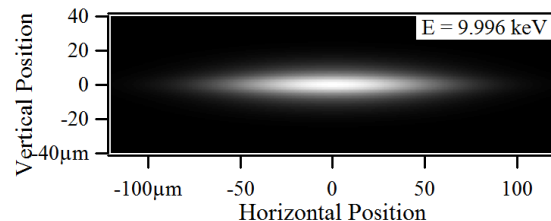
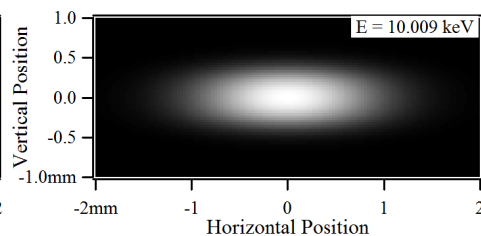
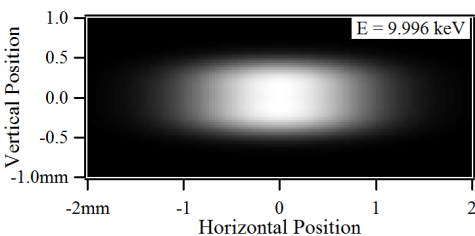
Test Optical Scheme



Intensity Distributions at ~10 keV

At 30-m from Undulator

In 1:1 Image Plane

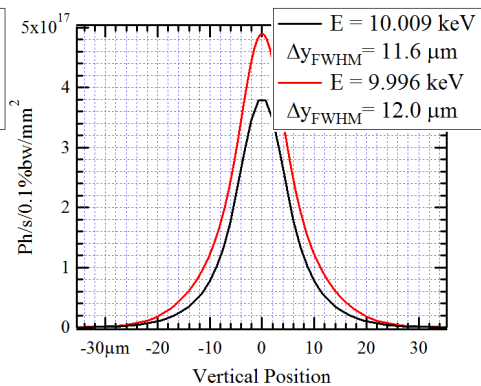
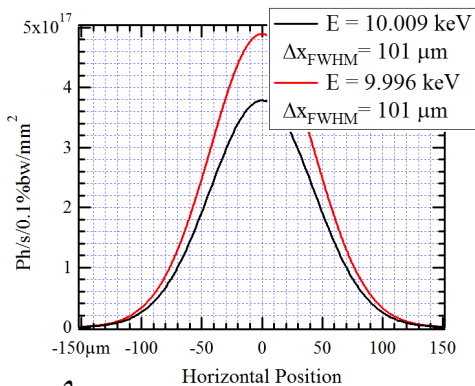
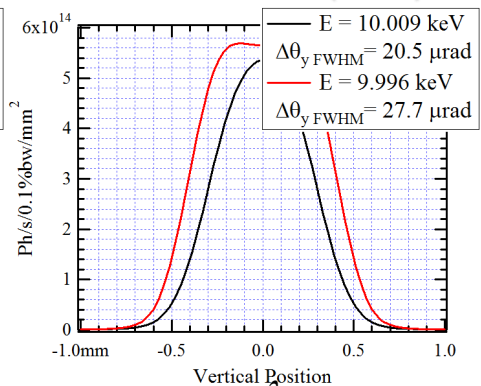
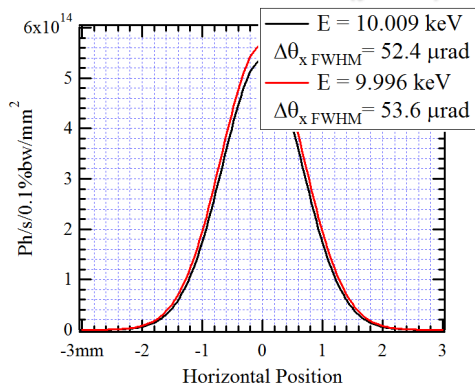


Horizontal Cuts ($y = 0$)

Vertical Cuts ($x = 0$)

Horizontal Cuts ($y = 0$)

Vertical Cuts ($x = 0$)



$$\sigma_x \sigma_x' \approx 97 \frac{\lambda}{4\pi}; \quad \sigma_y \sigma_y' \approx 5.7 \frac{\lambda}{4\pi}$$

...very far from Coherent Gaussian Beam !

Intensity Distributions of Focused Wiggler Radiation from Partially-Coherent Wavefront Propagation Calculations

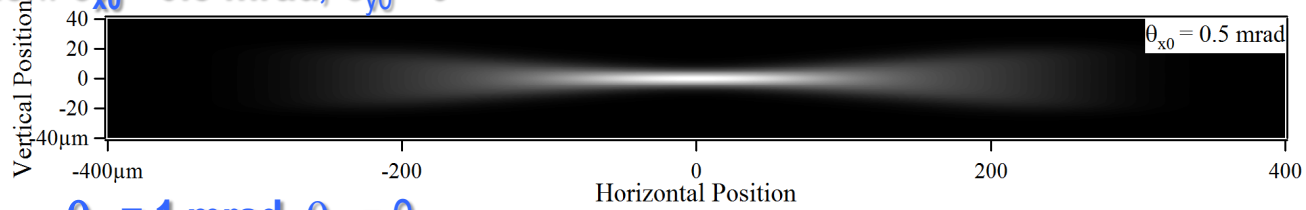
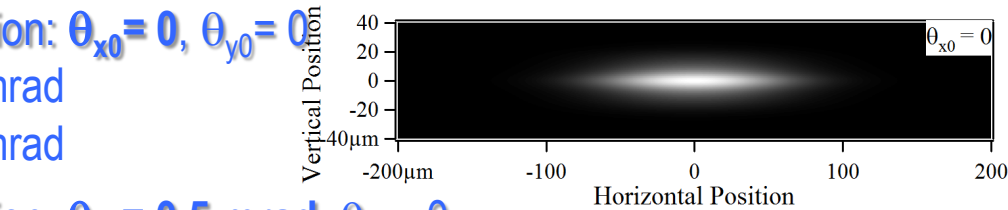
On-Axis Collection: $\theta_{x0} = 0, \theta_{y0} = 0$

$|\theta_x - \theta_{x0}| < 0.1 \text{ mrad}$

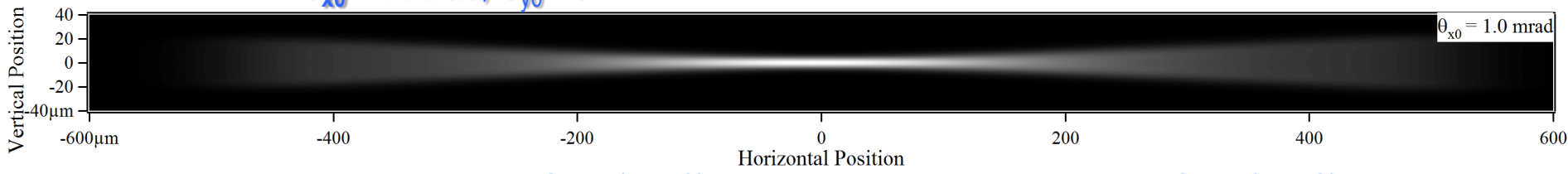
$|\theta_y - \theta_{y0}| < 0.1 \text{ mrad}$

1 : 1 Imaging Scheme with "Ideal Lens"

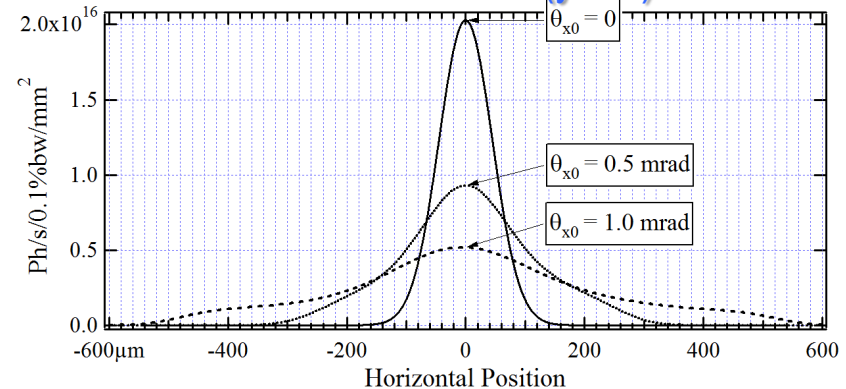
Off-Axis Collection: $\theta_{x0} = 0.5 \text{ mrad}, \theta_{y0} = 0$



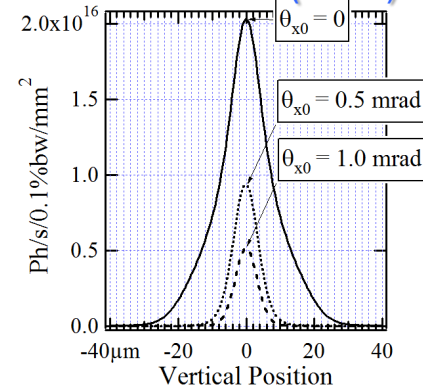
$\theta_{x0} = 1 \text{ mrad}, \theta_{y0} = 0$



Horizontal Cuts ($y = 0$)



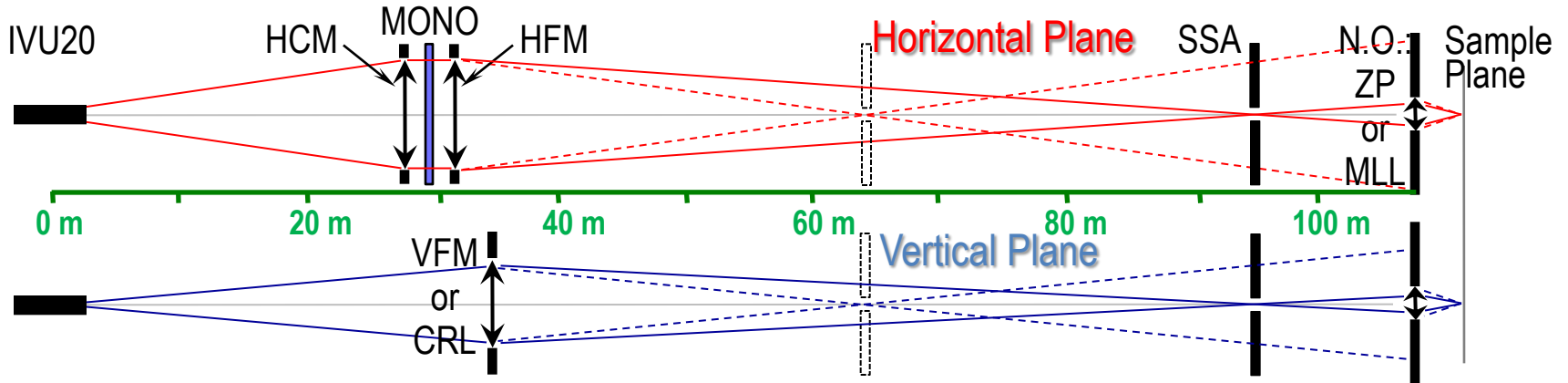
Vertical Cuts ($x = 0$)



NSLS-II Low-Beta Straight Section
 $I = 0.5 \text{ A}, \epsilon_x = 0.9 \text{ nm}, \epsilon_y = 8 \text{ pm}$

SCW40: $\lambda_u = 40 \text{ mm}, B_{\text{max}} = 3 \text{ T}, L = 1 \text{ m}$
 Photon Energy: $E_{\text{ph}} = 10 \text{ keV}$

NSLS-II Hard X-Ray Nanoprobe (HXN) Beamline Conceptual Optical Scheme



Y. Chu, H. Yan, K. Kaznatcheev

Approximations Used to Simulate Optical Elements:

Horizontal Collimating, Horizontal Focusing and Vertical Focusing **Mirrors** (HCM, HFM and VFM respectively), and **Nanofocusing Optics** (N.O.) simulated by “**Ideal**” **Lenses**.

Geometrical Apertures of all Mirrors, the Secondary Source Aperture (SSA), and the N.O. are **carefully respected**.

Monochromator (MONO) was assumed to be “**Ideal**”.

*Such approximations were used purposely, in order to “observe” pure effects related to **partial coherence** of the source, and to trace **losses on apertures**.*

Two possible SSA locations: at ~62 - 65 m and at ~92 - 94 m from undulator.

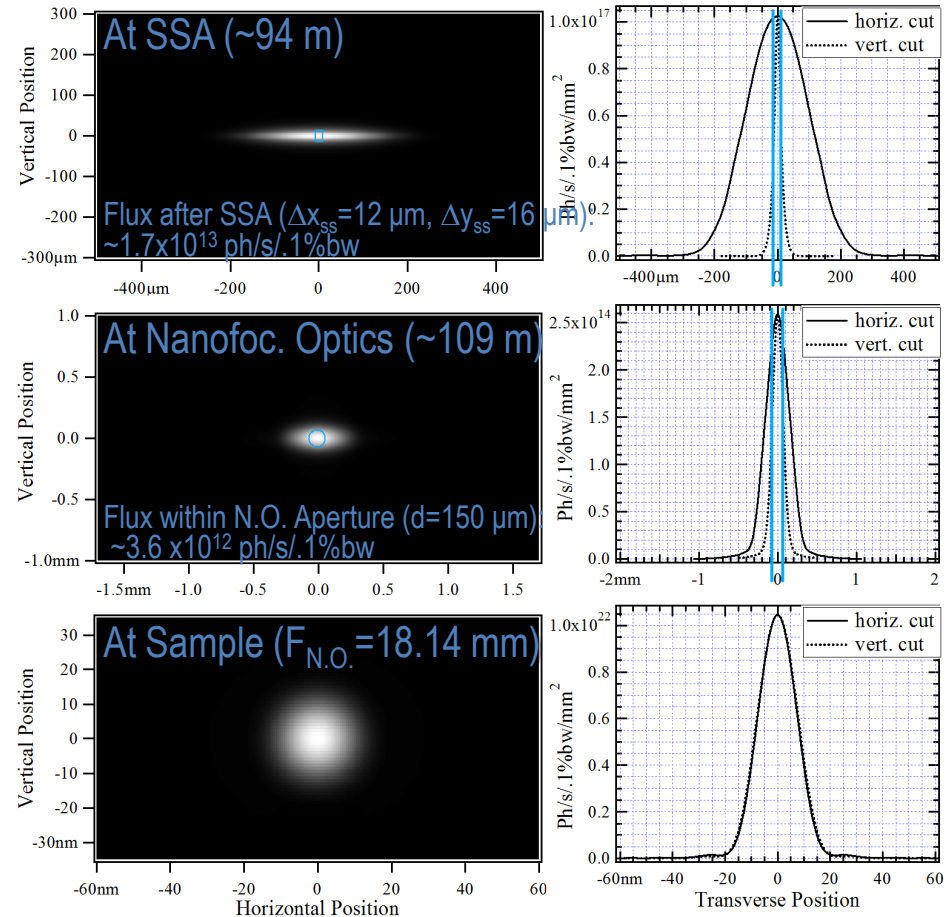
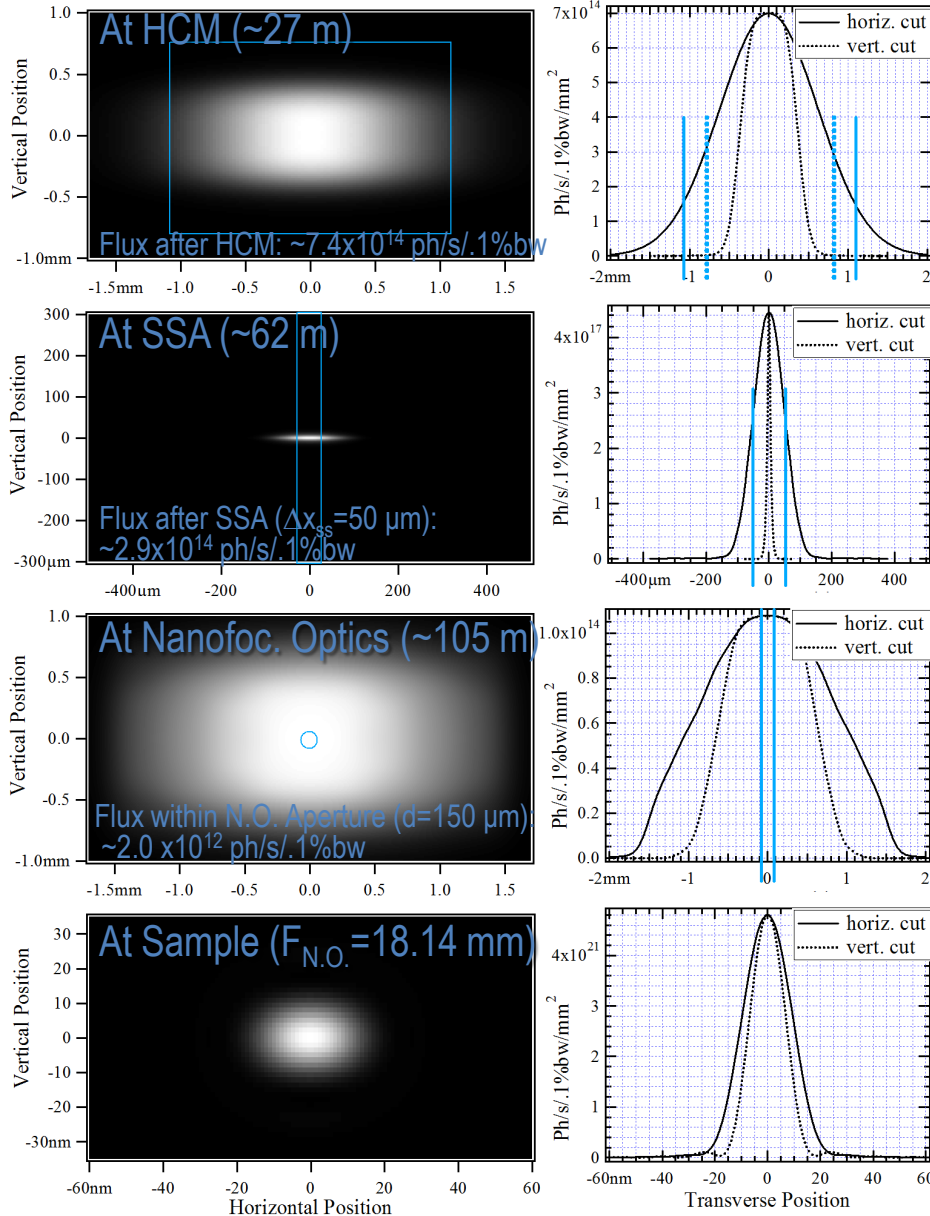
Two N.O. cases: $F = 18.14$ mm, $D = 150$ μm ; and $F = 42.33$ mm, $D = 350$ μm ($\Delta r \approx 15$ nm in both cases); $E_{\text{ph}} \approx 10$ keV

Intensity Distributions at Different Locations of HXN Beamline

Option with Secondary Source at 62 m

$I_e = 0.5 \text{ A}$
 $E_{ph} \approx 10 \text{ keV}$
 5th harmonic of IVU20 at $K \approx 1.5$

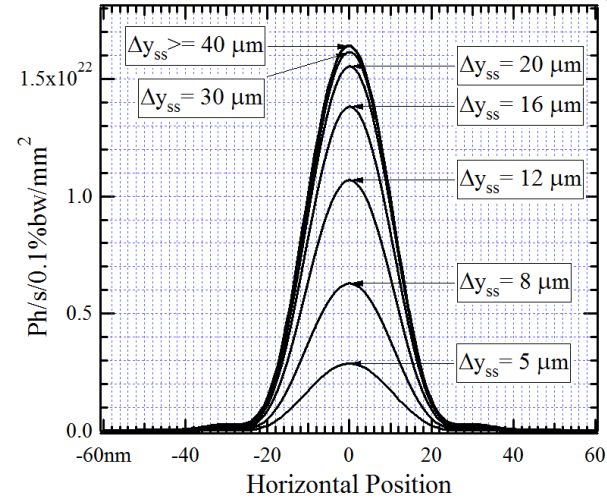
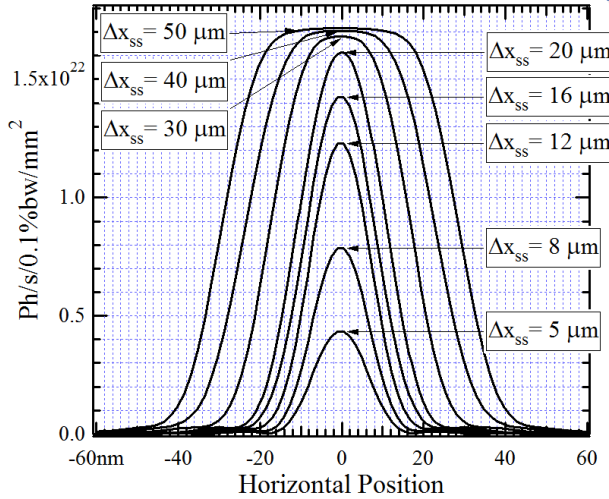
Option with Secondary Source at 94 m



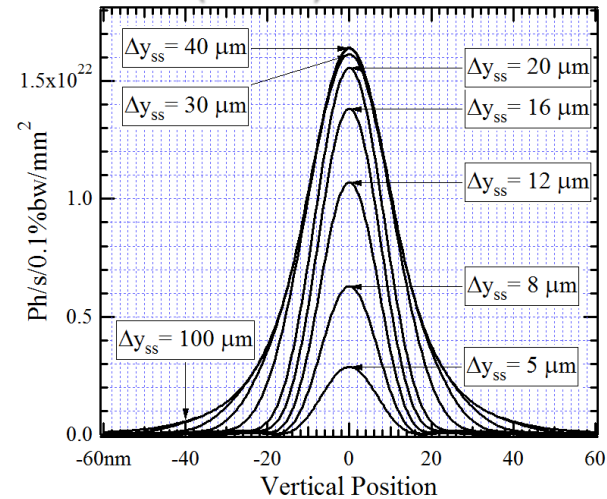
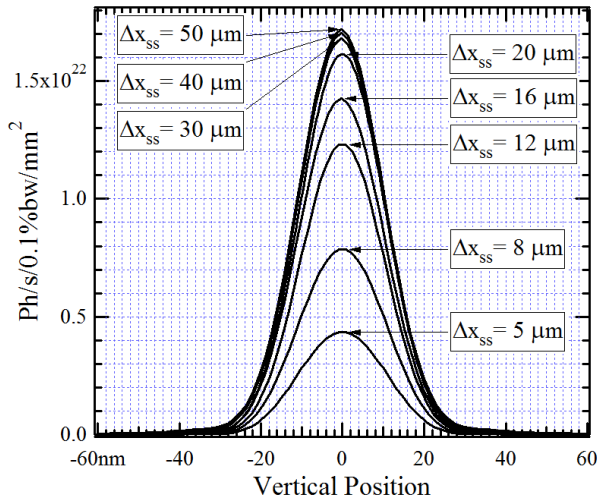
Intensity Distributions at Sample for Different Secondary Source Aperture Sizes at HXN (NSLS-II)

In Horizontal Median Plane ($y = 0$)

For Different Horizontal SSA Sizes (Δx_{ss}) For Different Vertical SSA Sizes (Δy_{ss})



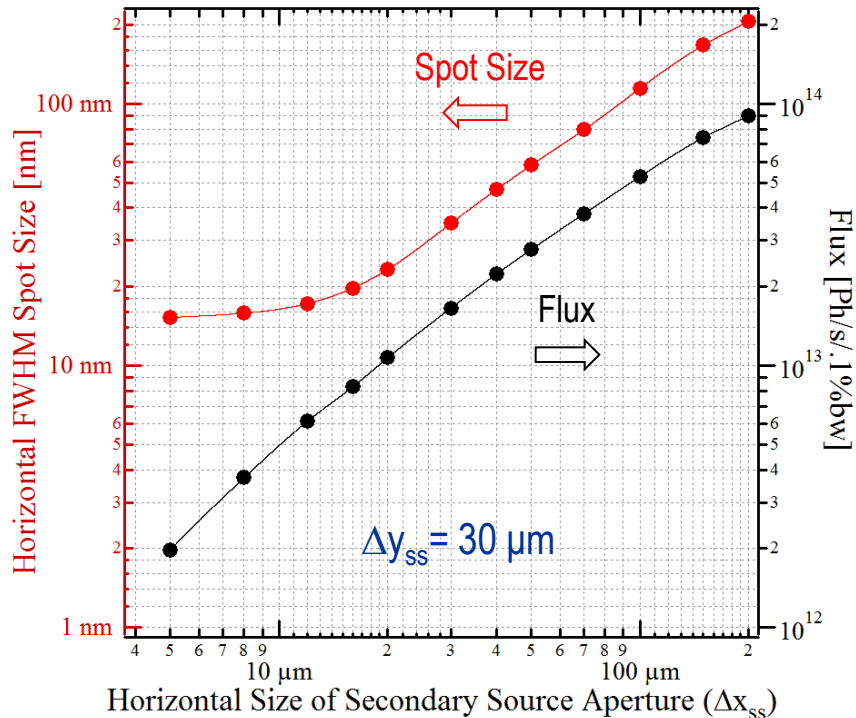
In Vertical Median Plane ($x = 0$)



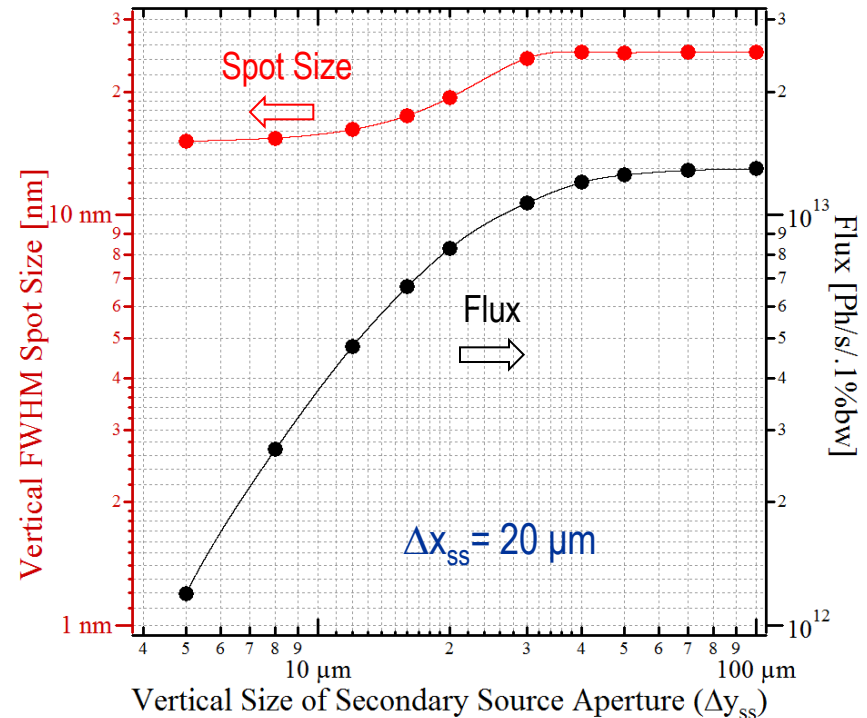
For Nanofocusing Optics with $F = 18.14$ mm, $D = 150 \mu m$ ($\Delta r \approx 15$ nm; $E_{ph} \approx 10$ keV)
SSA located at 94 m, Nanofocusing Optics at 109 m from Undulator

Final Focal Spot Size and Flux vs Secondary Source Aperture Size (HXN, NSLS-II)

Horizontal Spot Size and Flux vs Horizontal Secondary Source Aperture Size



Vertical Spot Size and Flux vs Vertical Secondary Source Aperture Size



Secondary Source Aperture located at 94 m from Undulator
 Spot Size and Flux calculated for Nanofocusing Optics simulated by Ideal Lens
 with $F = 18.14 \text{ mm}$, $D = 150 \mu\text{m}$ located at 15 m from Secondary Source (109 m from Undulator)

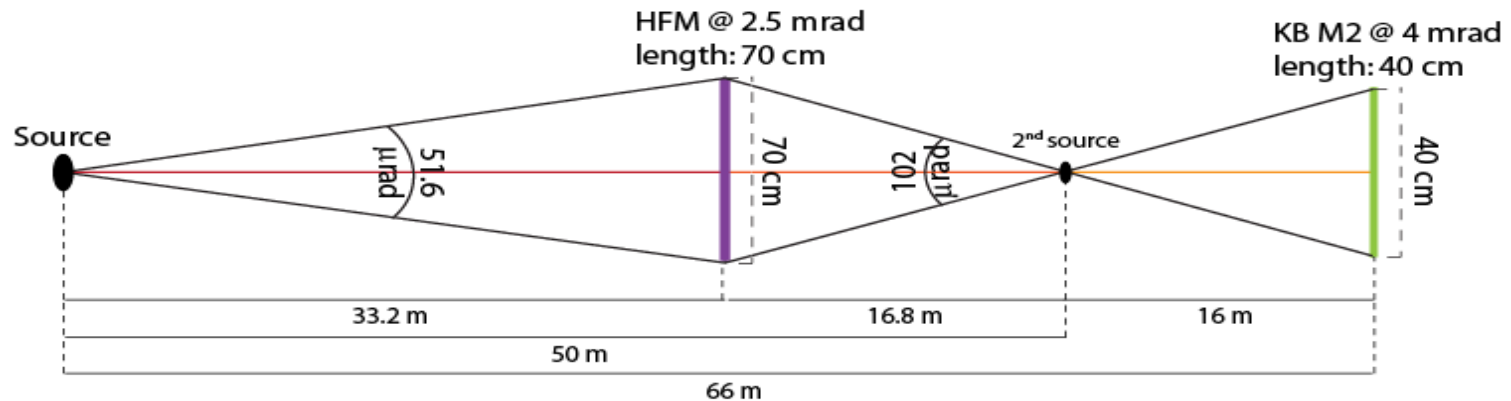
NSLS-II SRX Beamline Conceptual Optical Scheme

2 operation modes with 2 sets of KB's:

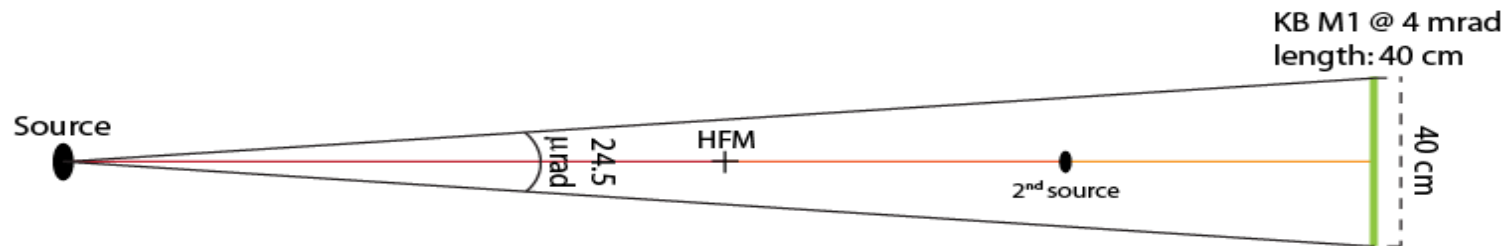
- High flux mode (with large mirrors)
- High resolution mode (diffraction limited)

J. Thieme
V. DeAndrade

Horizontal Plane



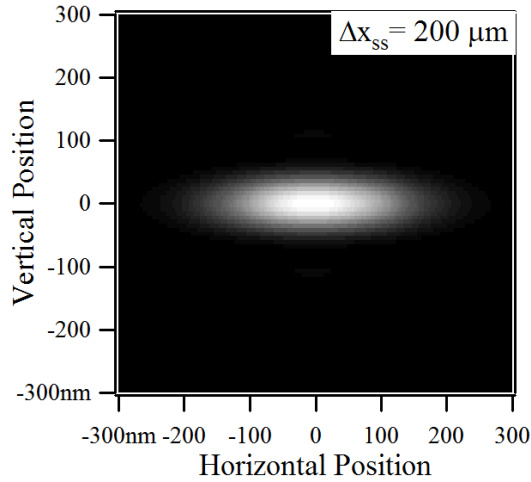
Vertical Plane



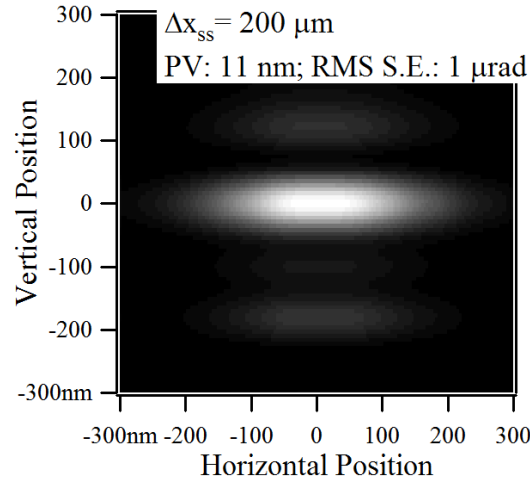
Preliminary Partially-Coherent Wavefront Propagation Simulation Results for SRX: Imperfect K-B Mirrors (I)

Intensity Distributions “at Sample”
at 200 μm Size of Secondary Source Aperture

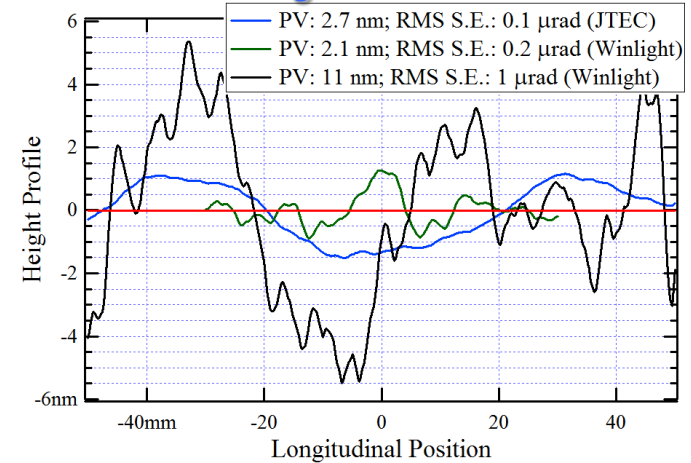
Perfect Optics (Ideal Lenses)



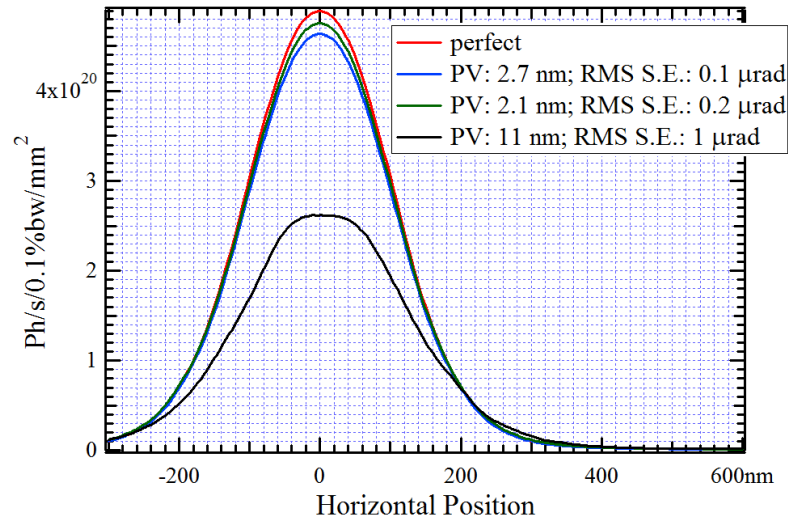
Imperfect Optics



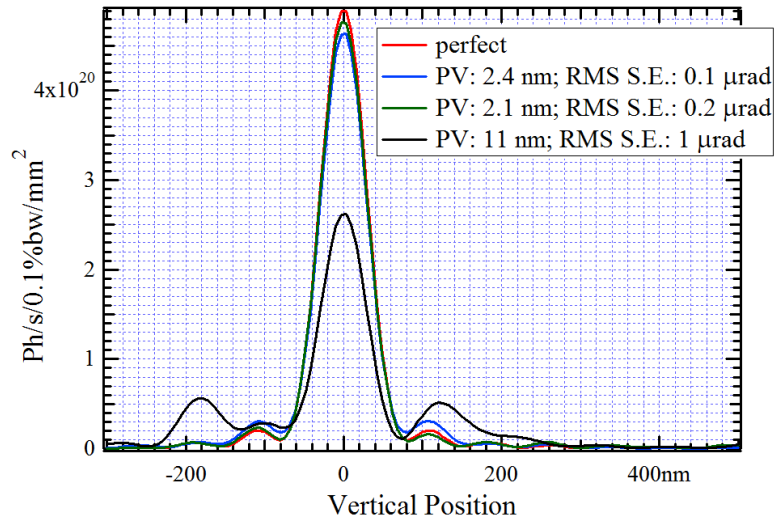
Imperfect Mirror
Height Profiles



Horizontal Cuts



Vertical Cuts

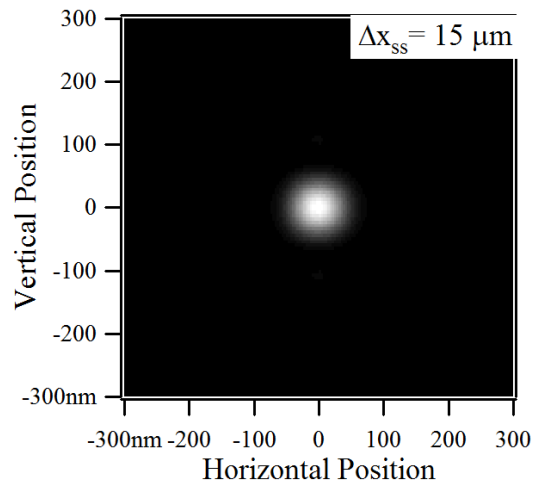


V. DeAndrade

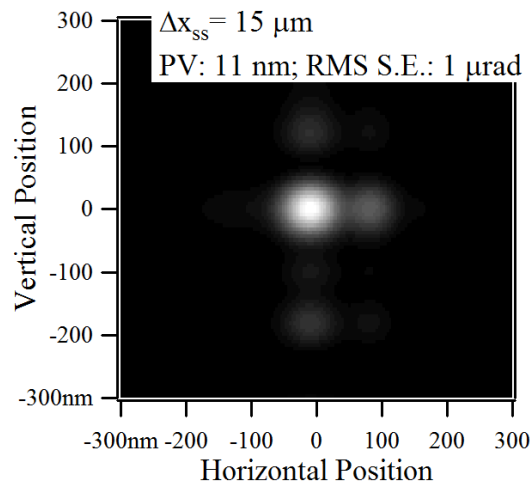
Preliminary Partially-Coherent Wavefront Propagation Simulation Results for SRX: Imperfect K-B Mirrors (II)

Intensity Distributions “at Sample”
at 15 μm Size of Secondary Source Aperture

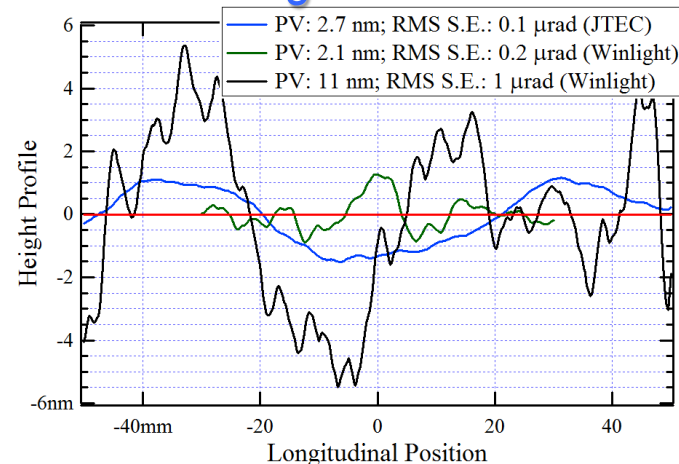
Perfect Optics (Ideal Lenses)



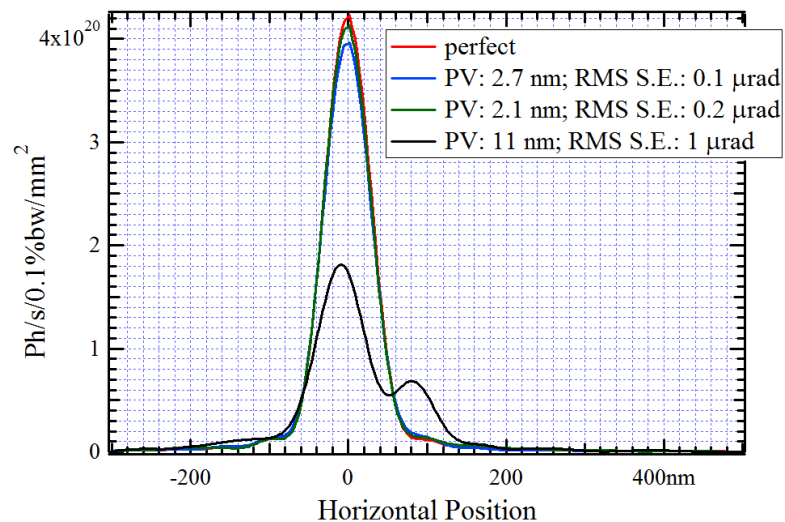
Imperfect Optics



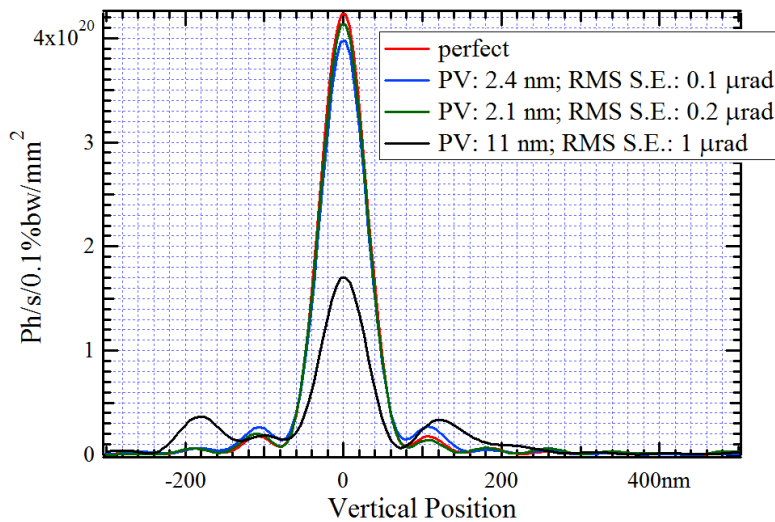
Imperfect Mirror
Height Profiles



Horizontal Cuts

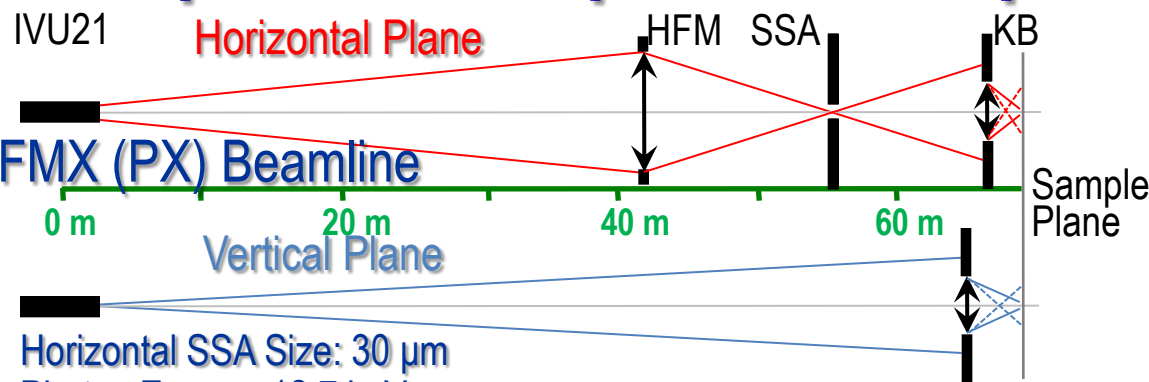


Vertical Cuts



V. DeAndrade

Intensity Distributions at Sample Taking Into Account Ellipsoidal Shapes and Slope Errors of KB Mirrors

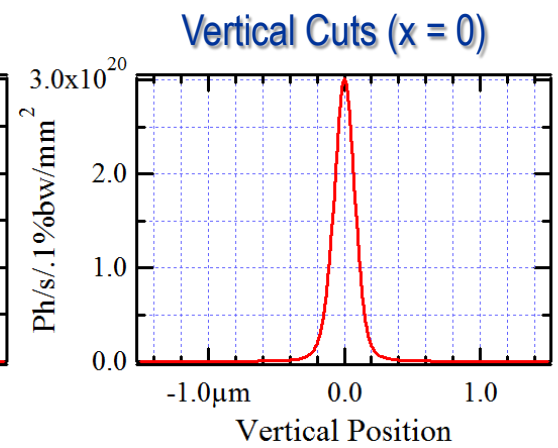
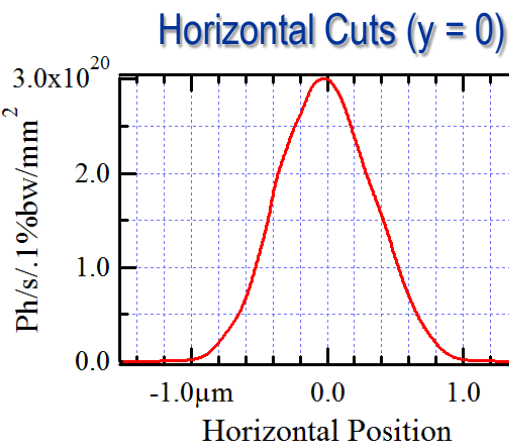
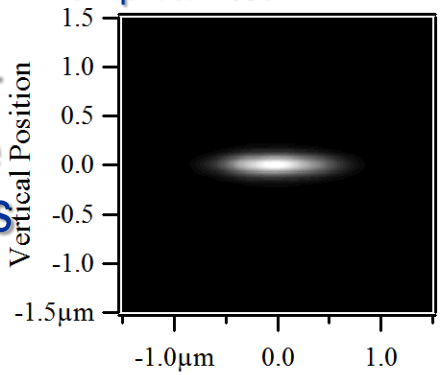


KB simulated using Grazing-Incidence "Thick Optical Element" Propagator based on Local Ray-Tracing.

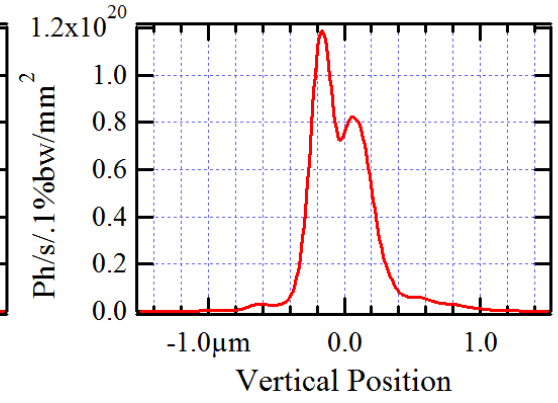
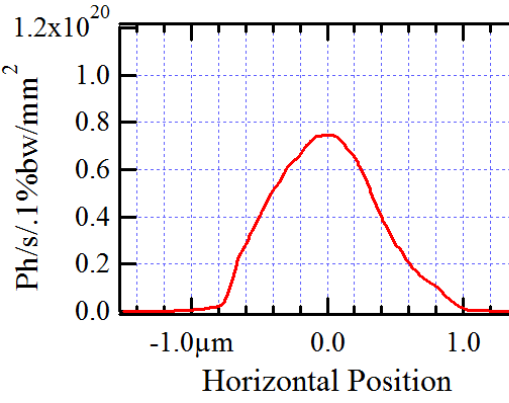
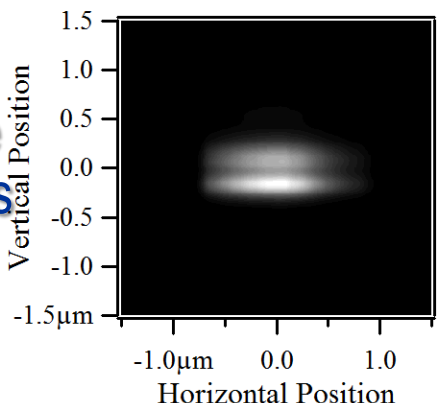
KB Surface Height Error simulated by corresponding Phase Shifts ("Masks") in Transverse Plane at Mirror Locations.

Horizontal SSA Size: 30 μm
 Photon Energy: 12.7 keV
 Flux at Sample: $\sim 5.4 \times 10^{13}$ ph/s/.1%bw

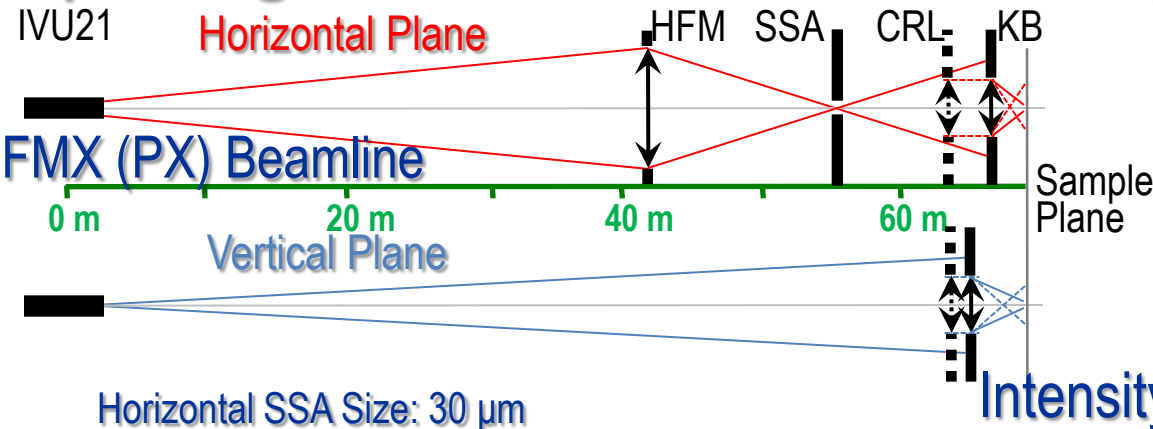
Without Mirror Surface Slope (/Height) Errors



With Mirror Surface Slope (/Height) Errors



Using CRLs for Producing “Large Spot” at Sample (taking into account Mirror Shape and Slope Error)



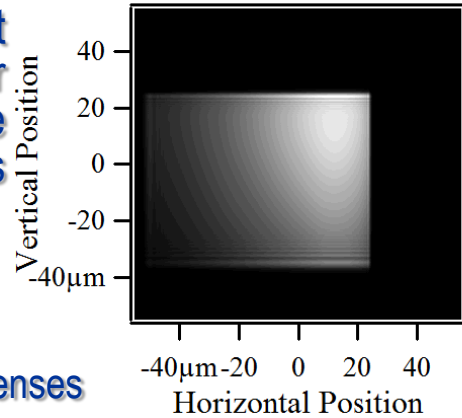
Source:

Electron Current: 0.5 A
Horizontal Emittance: 0.55 nm (“ultimate”)
Vertical Emittance: 8 pm
Undulator: IVU21 – 1.5 m centered at +1.25 m from Low-Beta Straight Section Center

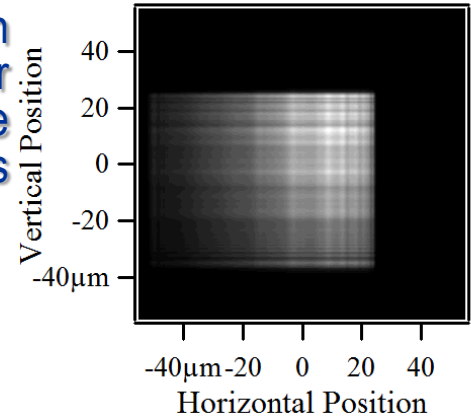
Horizontal SSA Size: 30 μm
Photon Energy: 12.7 keV

Intensity Distributions at Sample

Without Mirror Slope Errors



With Mirror Slope Errors



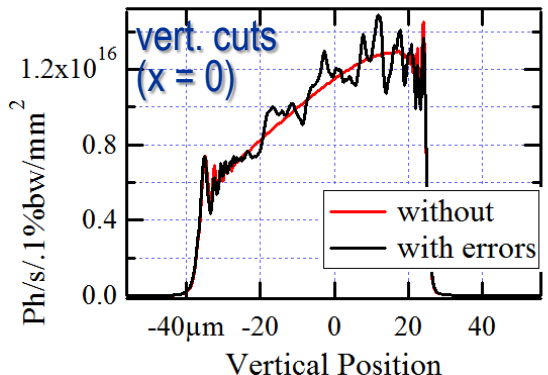
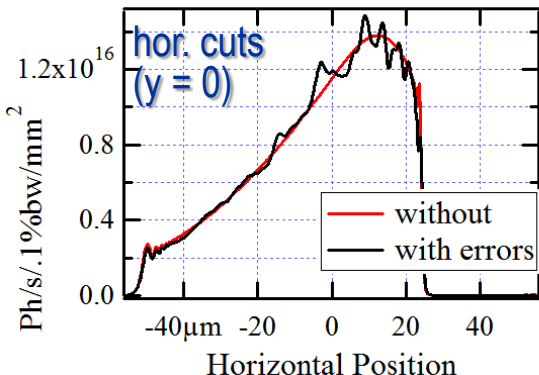
CRL “Transfocator”:

8 Horizontally + 3 Vertically-Focusing Be Lenses

$R_{\text{min}} = 200 \mu\text{m}$
 $F_h \approx 5.9 \text{ m}, F_v \approx 15.8 \text{ m}$
Geom. Ap.: 1 mm x 1 mm

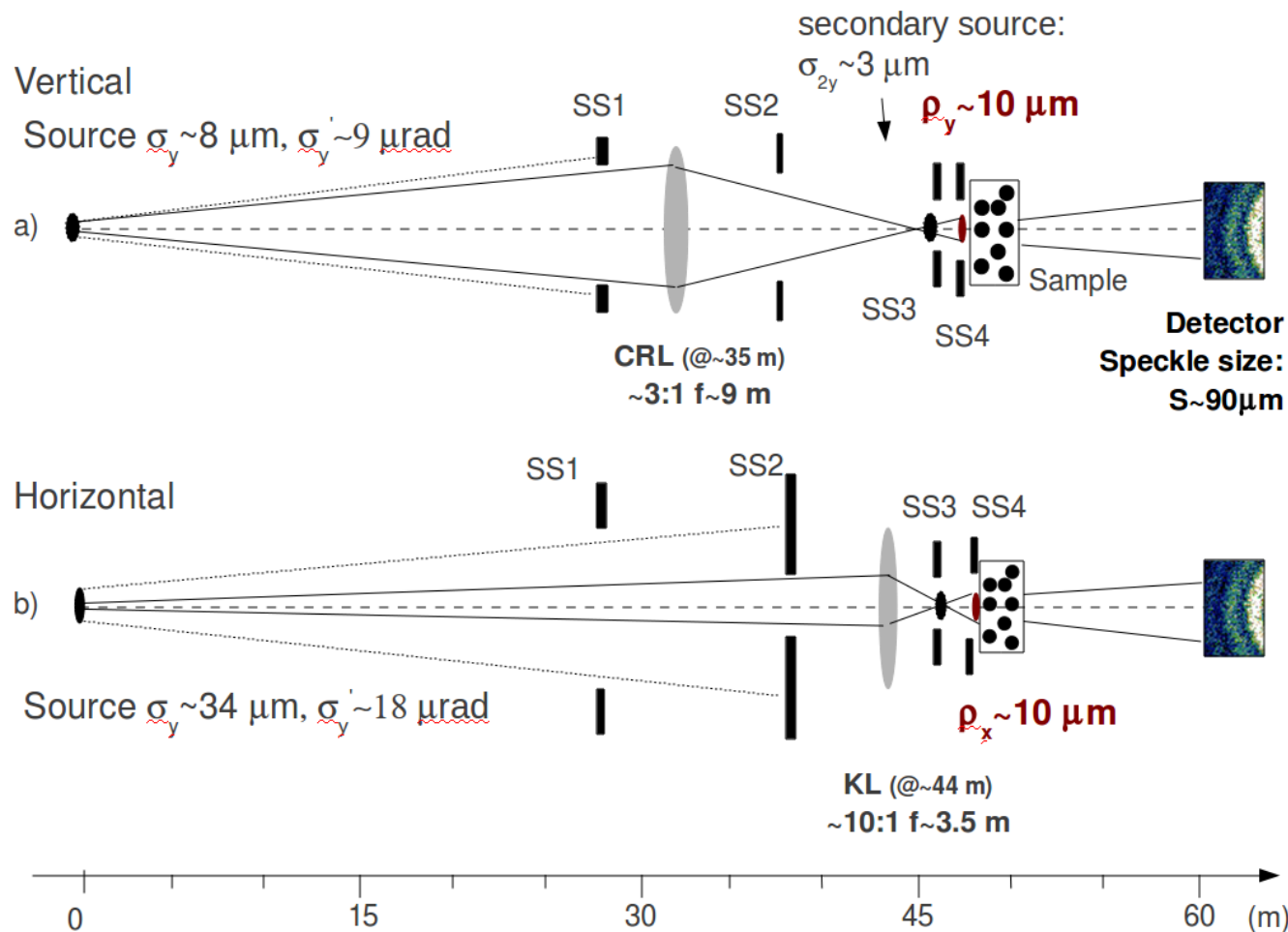
Located at 0.75 m before VKB edge (10 m after SSA)

Flux Losses at CRL: ~ 1.6 times



NSLS-II Coherent Hard X-Ray (CHX) Beamline Conceptual Optical Scheme

A. Fluerasu, L. Wiegart, K. Kaznatcheev, L. Berman



Partially-Coherent Wavefront Propagation Calculations for CHX

(I) Intensity Distributions in the Case of: $\Delta S_{1x} = 44 \mu\text{m}$, $\Delta S_{1y} = 250 \mu\text{m}$

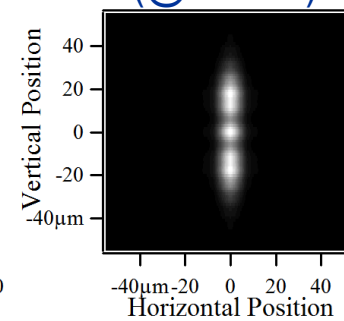
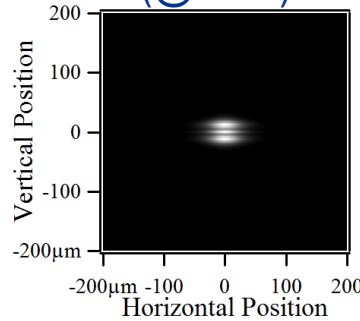
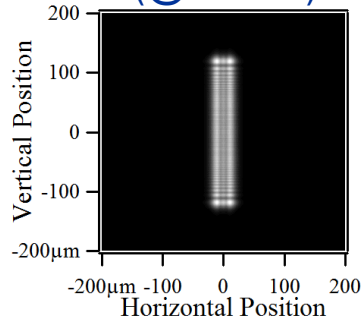
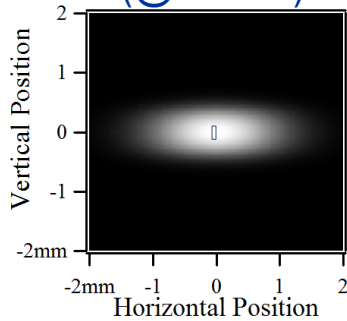
Before SS1
(@33.5 m)

Before CRL
(@35.3 m)

Before KL
(@44 m)

At Sample
(@48.5 m)

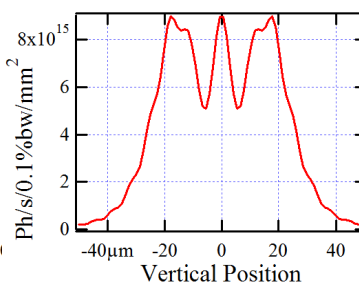
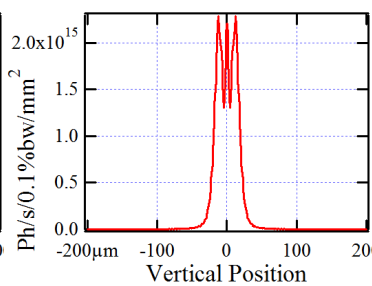
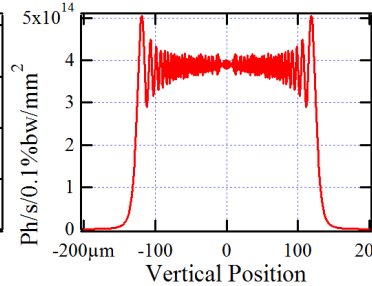
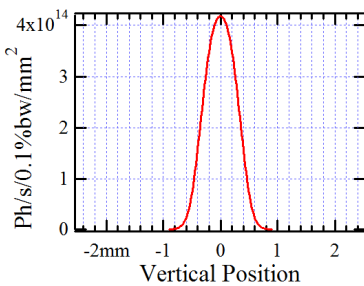
E=10 keV



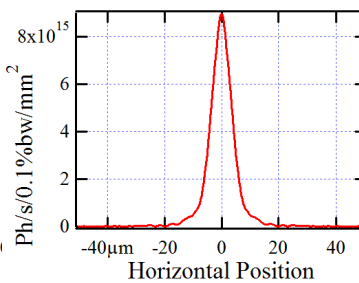
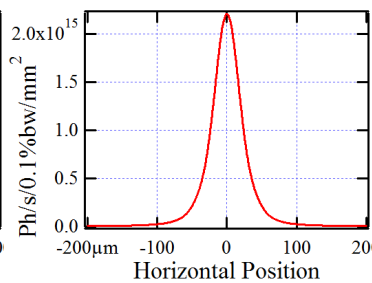
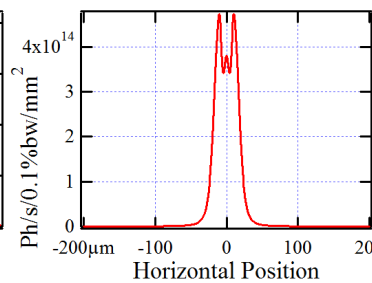
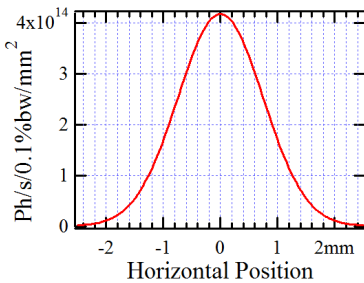
Be 1D CRL: $N = 9$, $A_{\text{geom}} = 1 \text{ mm}$
 $R_{\text{min}} = 0.5 \text{ mm}$, $F_y = 8.152 \text{ m}$

$F_{\text{KLx}} \approx 3.5 \text{ m}$
Vertical Cuts

Flux: $4 \times 10^{13} \text{ ph/s/0.1\%bw}$



Horizontal Cuts



Partially-Coherent Wavefront Propagation Calculations for CHX

(II) Intensity Distributions in the Case of: $\Delta S_{1x} = 44 \mu\text{m}$, $\Delta S_{1y} = 100 \mu\text{m}$

Before SS1
(@33.5 m)

Before CRL
(@35.3 m)

Before KL
(@44 m)

At Sample
(@48.5 m)

E=10 keV

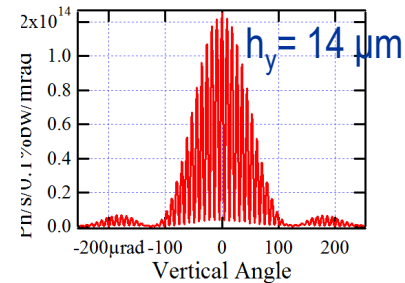
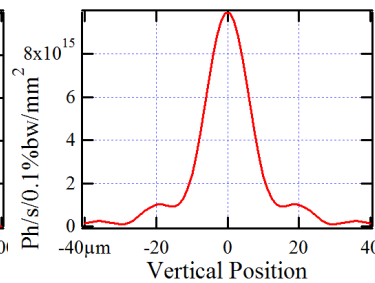
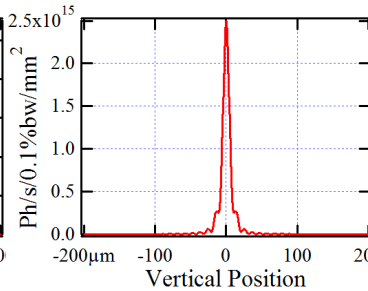
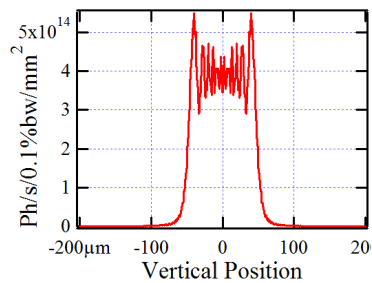
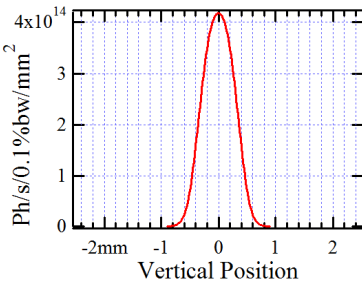
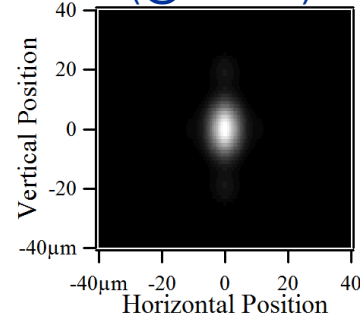
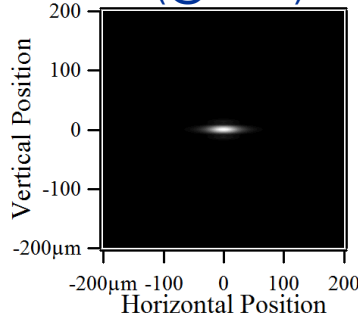
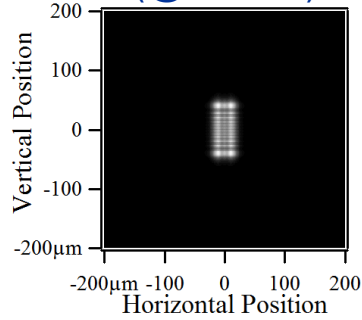
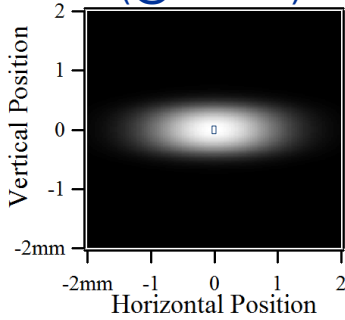
After 2 Slits
placed at Sample

Observation in Far Field
Slit Size: $1 \mu\text{m}$

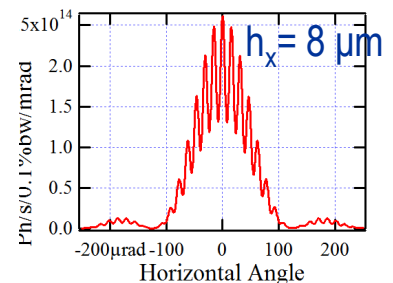
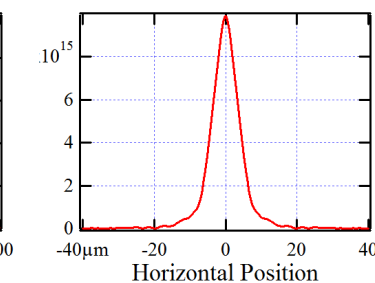
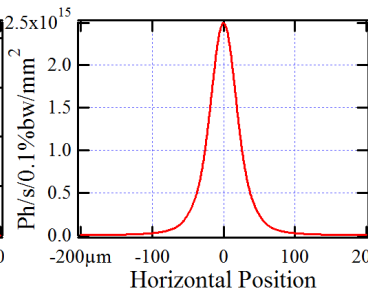
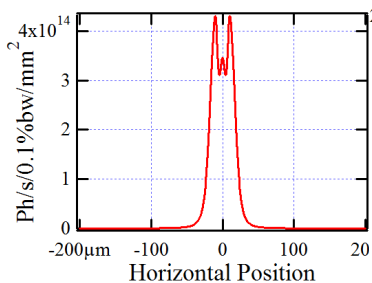
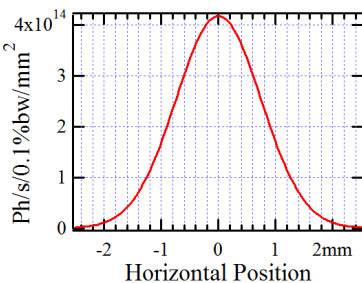
Be 1D CRL: $N = 9$, $A_{\text{geom}} = 1 \text{ mm}$
 $R_{\text{min}} = 0.5 \text{ mm}$, $F_y = 8.152 \text{ m}$

$F_{\text{KLx}} \approx 3.5 \text{ m}$
Vertical Cuts

Flux: $1.6 \times 10^{12} \text{ ph/s/0.1\%bw}$



Horizontal Cuts



Partially-Coherent Wavefront Propagation Calculations for CHX

(III)

Before SS1
(@33.5 m)

Before CRL
(@35.8 m)

Intensity Distributions in the Case of:

$$\Delta S_{1x} = 44 \mu\text{m}, \Delta S_{1y} = 1 \text{ mm}$$

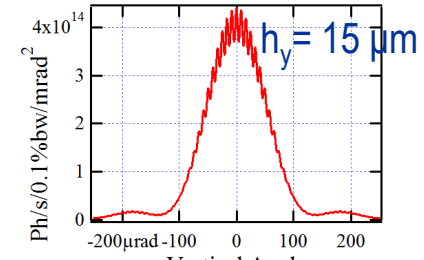
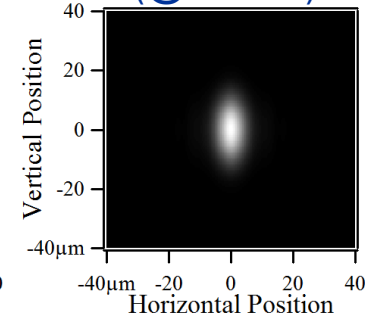
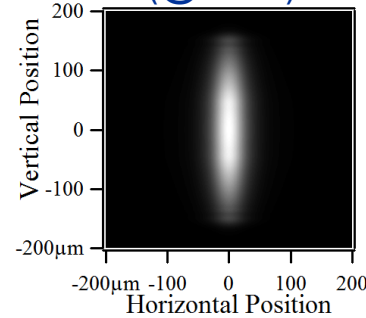
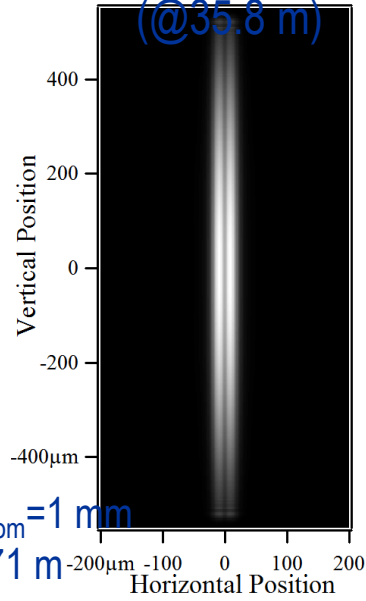
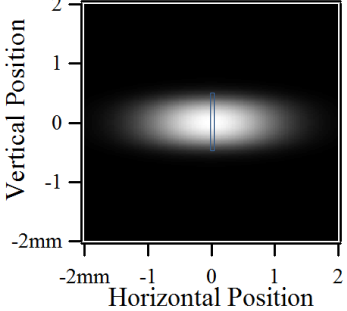
E=10 keV

Before KL
(@44 m)

At Sample
(@48.5 m)

After 2 Slits
placed at Sample

Observation in Far Field
Slit Size: 1 μm

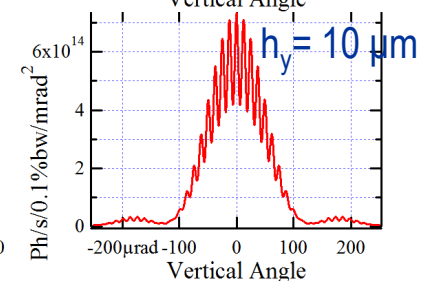
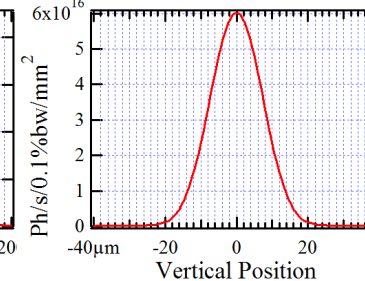
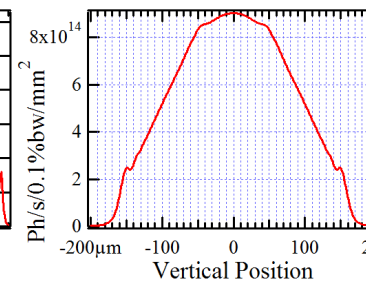
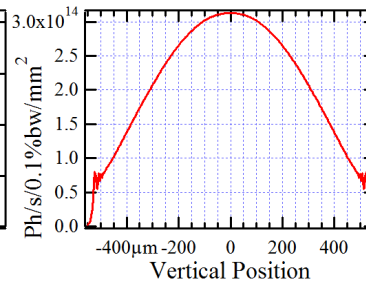
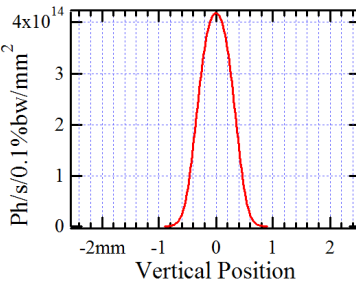


Be 1D CRL: N = 8, $A_{\text{geom}} = 1 \text{ mm}$
 $R_{\text{min}} = 0.5 \text{ mm}, F_y = 9.171 \text{ m}$

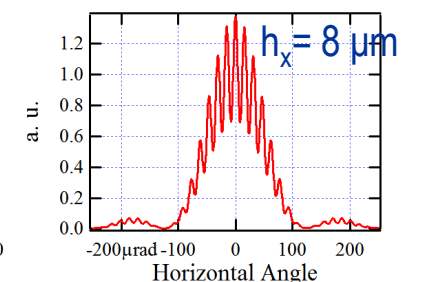
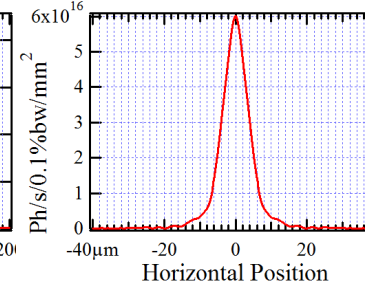
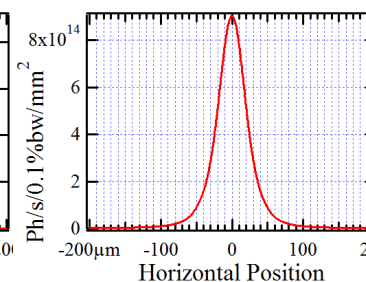
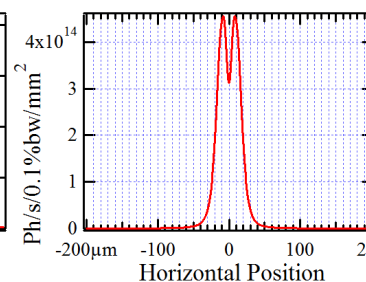
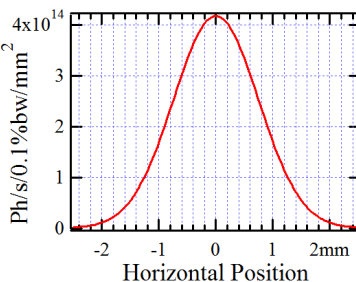
$F_{\text{KLx}} \approx 3.5 \text{ m}$

Flux: $10^{13} \text{ ph/s/0.1\%bw}$

Vertical Cuts



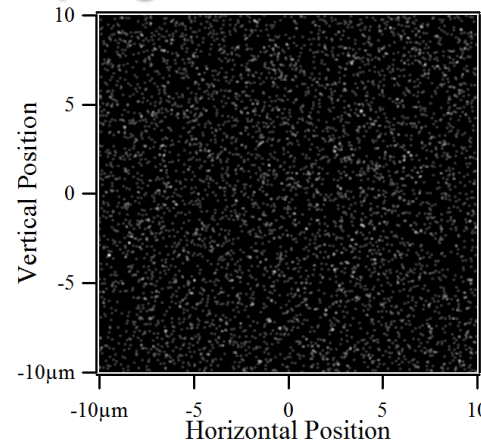
Horizontal Cuts



Partially-Coherent Wavefront Propagation Calculations for CHX

(IV) Diffraction / Scattering from Test Sample

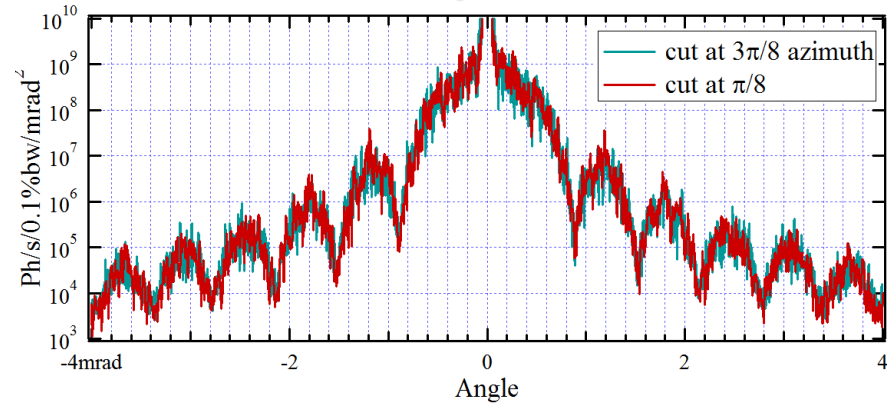
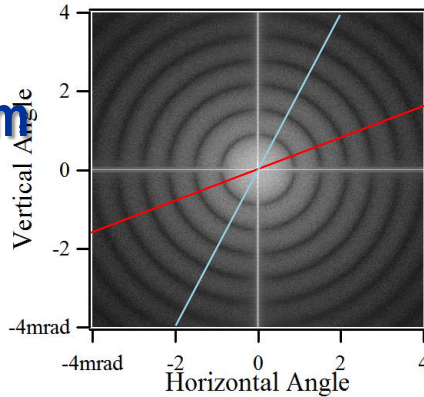
5000 "Silica Spheres", $d \approx 200$ nm



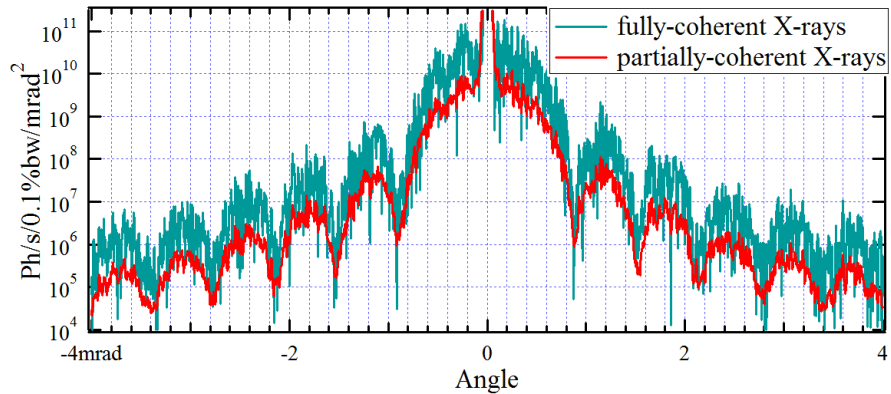
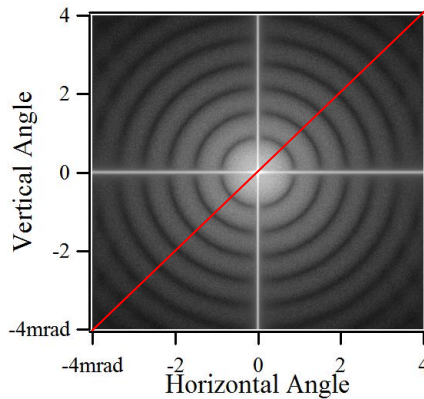
Sample data from Andrei Fluerasu

Angular Distribution of Scattered X-Rays at E=10 keV

$$\Delta S_{1x} = 44 \mu\text{m}$$
$$\Delta S_{1y} = 100 \mu\text{m}$$

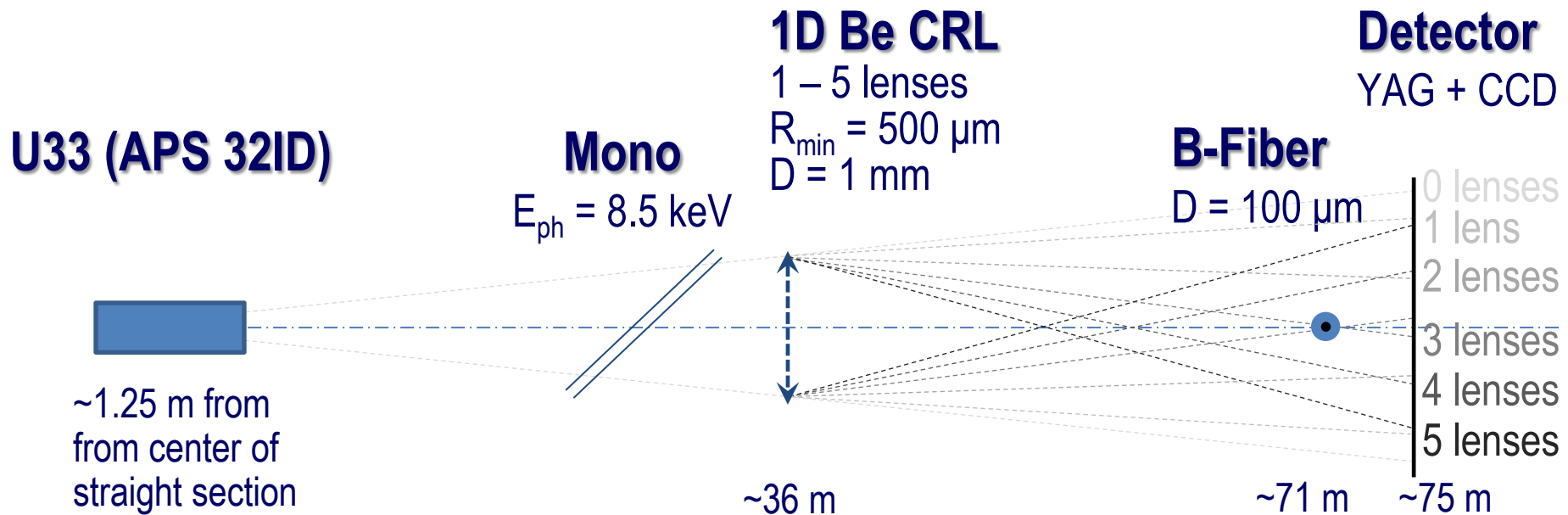


$$\Delta S_{1x} = 44 \mu\text{m}$$
$$\Delta S_{1y} = 1 \text{ mm}$$



Optical Scheme of Wavefront Preservation Test Experiments with CRL and a Boron Fiber Probe

APS, Dec. 2011

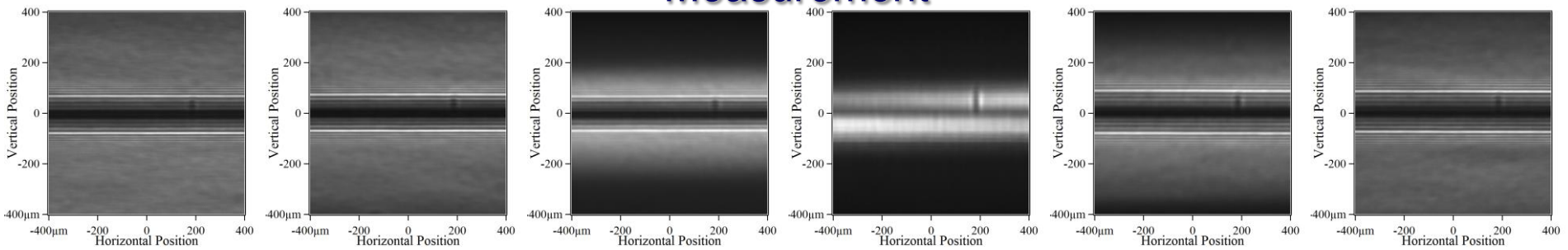


- V. Kohn, I. Snigireva and A. Snigirev, “Direct measurement of transverse coherence length of hard X-rays from interference fringes”, Phys. Rev. Lett., 2000, vol.85(13), p.2745.
- A. Snigirev, V. Kohn, I. Snigireva, B. Lengeler, “A compound refractive lens for focusing high-energy X-rays”, Nature, 1996, vol.384, p.49.
- New generation CRL from B. Lengeler et al.

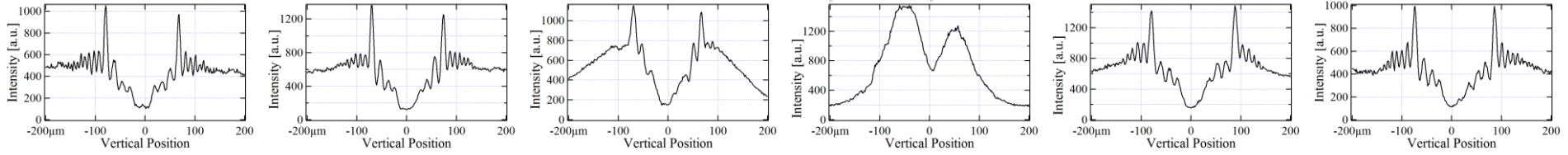
Intensity Distributions in B-Fiber Based Interference Scheme for Different Numbers of CRL in Optical Path

no lenses 1 lens 2 lenses 3 lenses 4 lenses 5 lenses

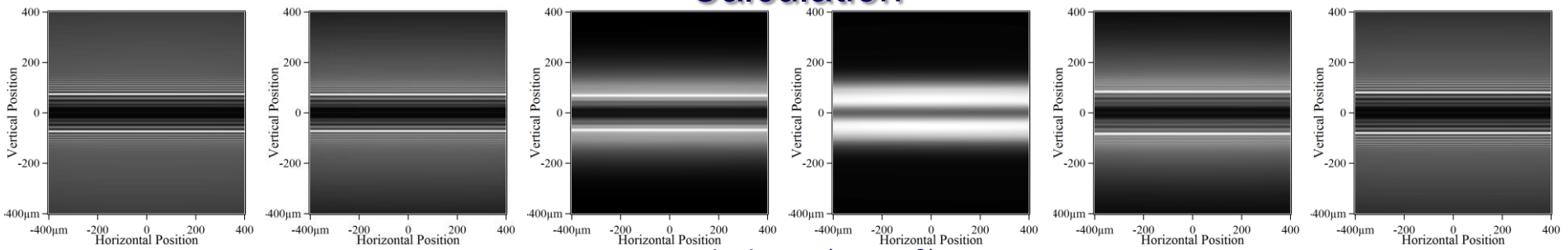
Measurement



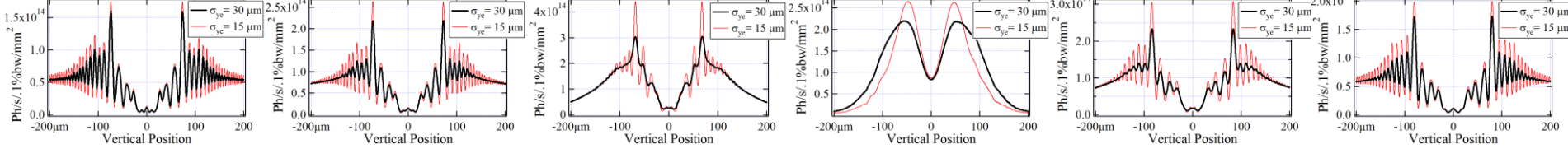
vertical cuts (at x = 0)



Calculation



vertical cuts (at x = 0)



Simulations for FEL: SASE Pulse Profiles and Spectra at FEL Exit

E-Beam: $E = 1 \text{ GeV}$ $\sigma_{te} \sim 200 \text{ fs}$
 $I_{peak} = 1.5 \text{ kA}$ $\varepsilon_x = \varepsilon_y = 1.2 \pi \text{ mm-mrad}$

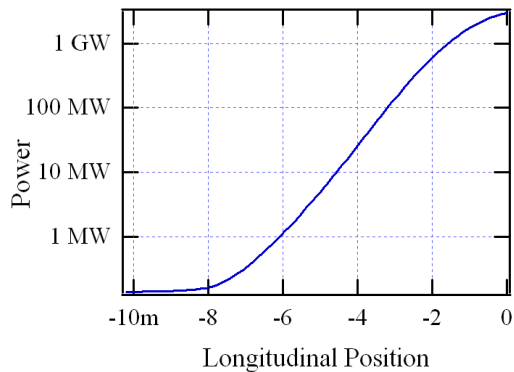
$P_{max\ ssed} \sim 50 \text{ kW}$
 $\sigma_{t\ seed} \sim 25 \text{ fs}$

Undulator: $K \sim 2.06$
 $\lambda_u = 30 \text{ mm}$
 $L_{tot} \sim 5 \times 2 \text{ m}$
 $\hbar\omega_0 = 100.15 \text{ eV}$

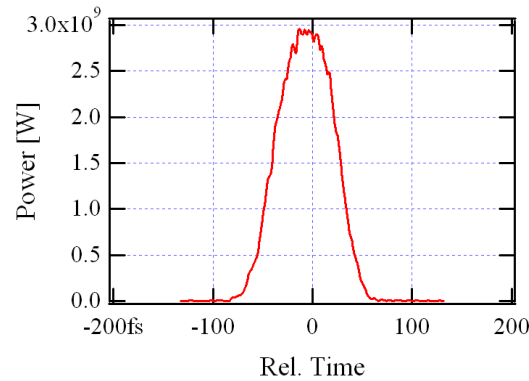
GENESIS
(integrated to SRW)

A: Seeded FEL operation

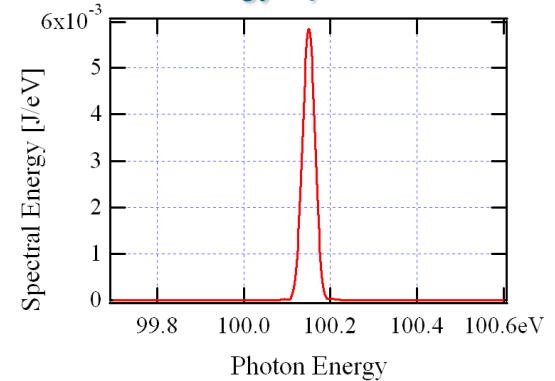
Peak Power vs Long. Position



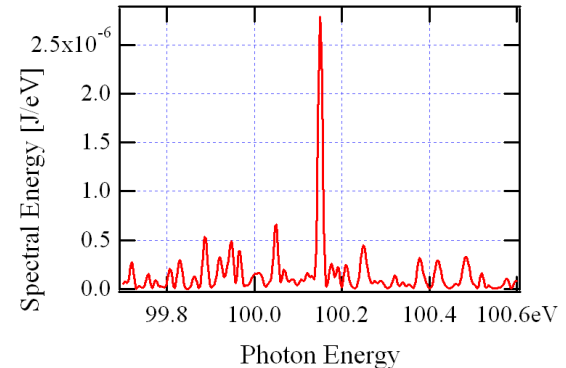
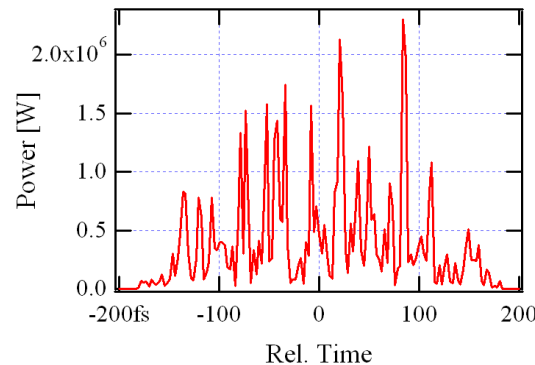
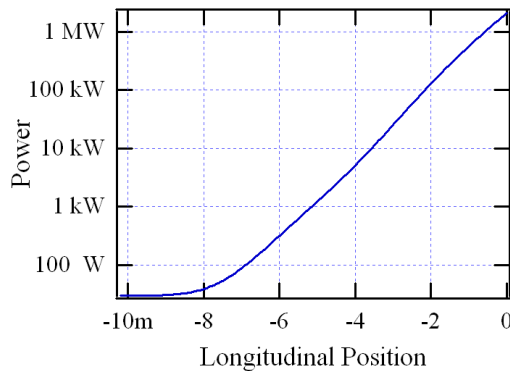
Power vs Time



Energy Spectrum



B: SASE (not saturated)

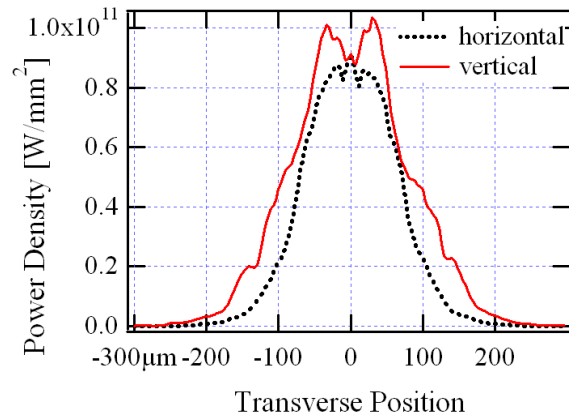


Simulations for FEL: SASE Intensity Distributions at FEL Exit

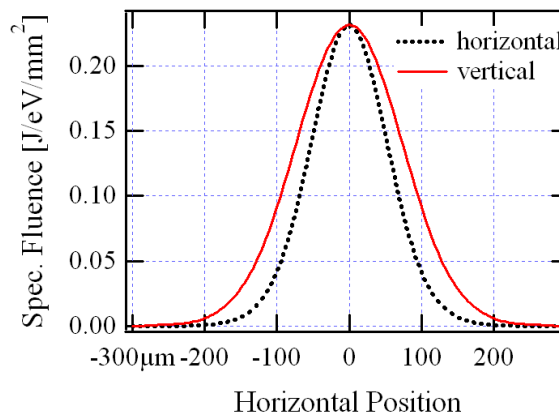
GENESIS
(integrated to SRW)

A: Seeded FEL operation

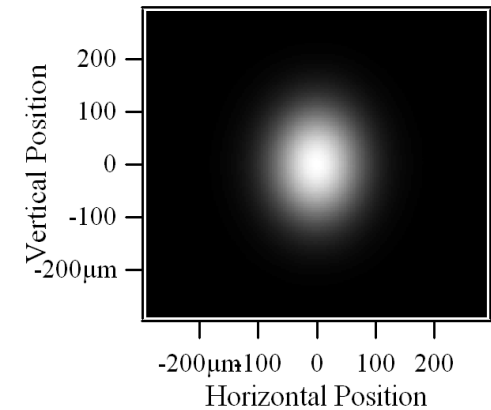
Power Density Cuts at Pulse Center



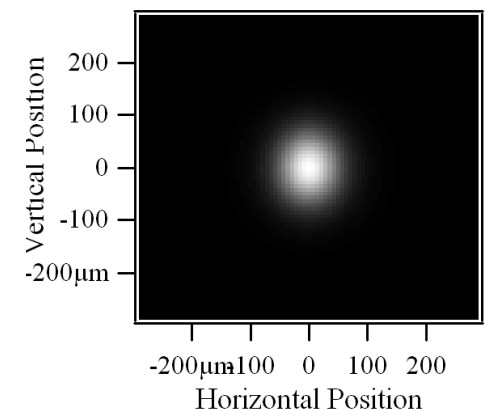
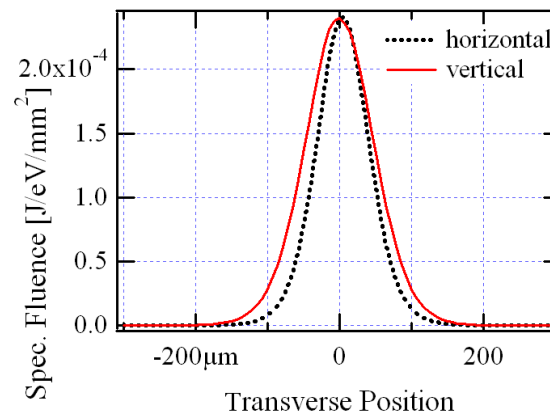
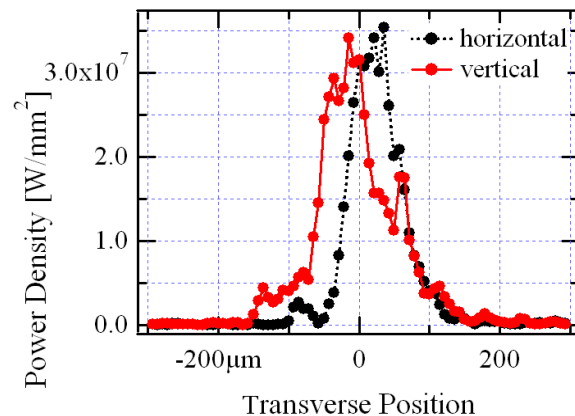
Peak Spectral Fluence Transverse Cuts



Fluence



B: SASE (not saturated)



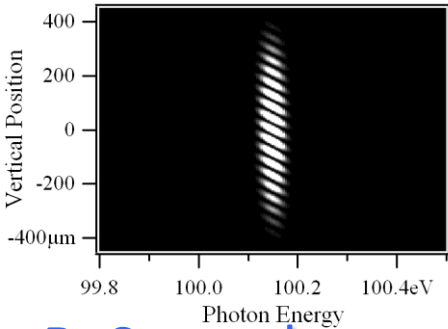
Time-Dependent FEL Wavefront Propagation Simulation: Pulse Characteristics in Image Plane of a 2-Slit Interferometer with a Grating

E-Beam: $E = 1 \text{ GeV}$ $\sigma_{te} \sim 200 \text{ fs}$, $\varepsilon_x = \varepsilon_y = 1.2 \pi \text{ mm-mr}$
 $I_{peak} = 1.5 \text{ kA}$

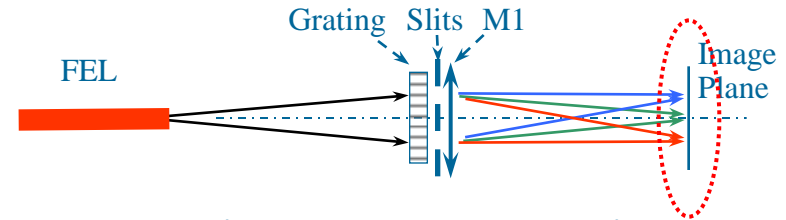
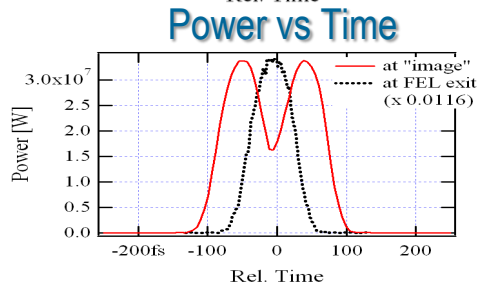
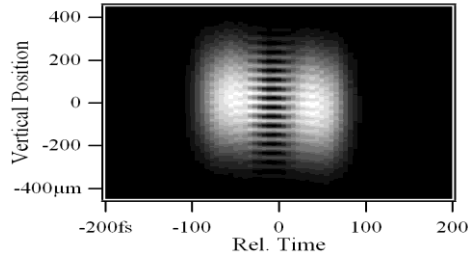
Undulator: $\lambda_u = 30 \text{ mm}$, $L_{tot} \sim 5 \times 2 \text{ m}$, $K \sim 2.06$

A: Seeded

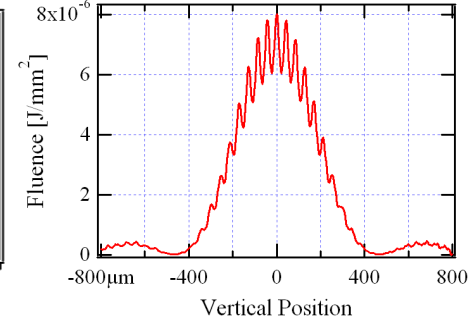
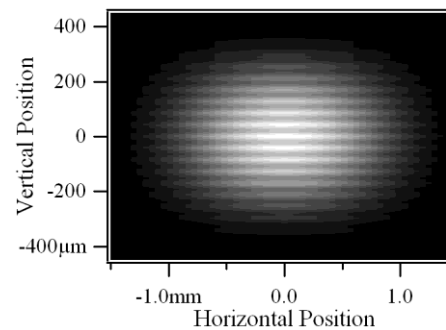
Spectral Fluence vs Photon Energy and Vertical Position (at $x = 0$)



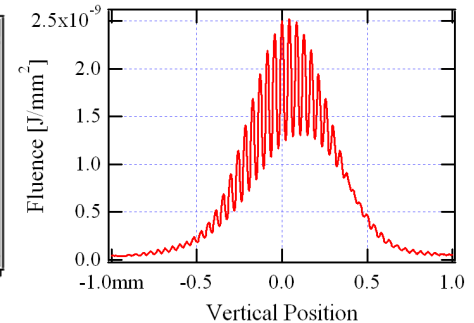
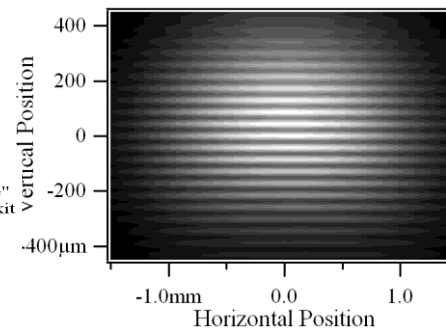
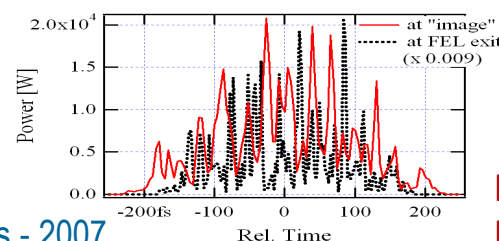
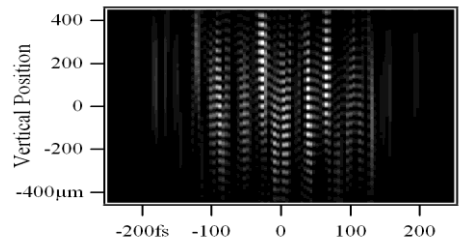
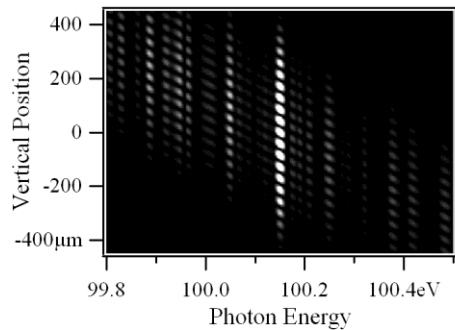
Power Density vs Time and Vertical Position (at $x = 0$)



Fluence (Time-Integrated Intensity) vs Horiz. and Vert. Positions vs Vert. Position (at $x = 0$)

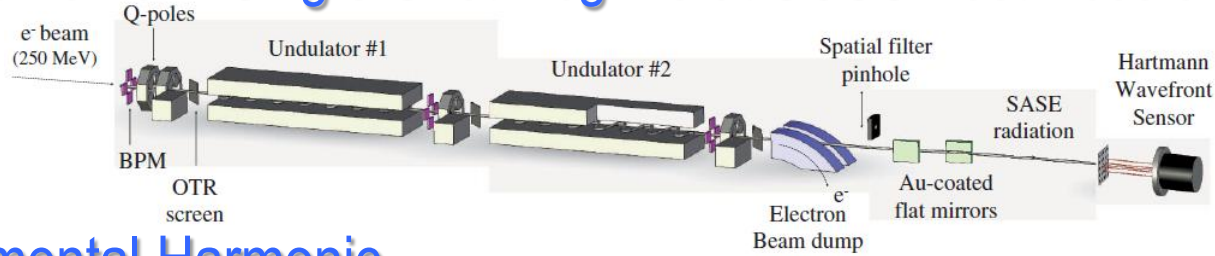


B: Started from noise



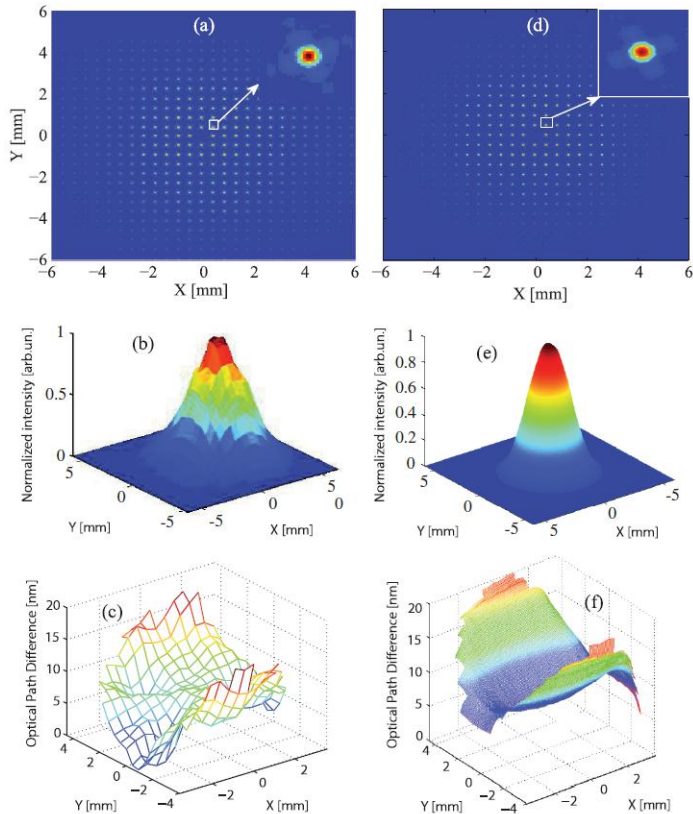
Extension of Hartmann Wavefront Sensor Method To Probe Transverse Coherence Over Wavefront

Measurements in Single-Shot Regime at SCSS Test Accelerator FEL



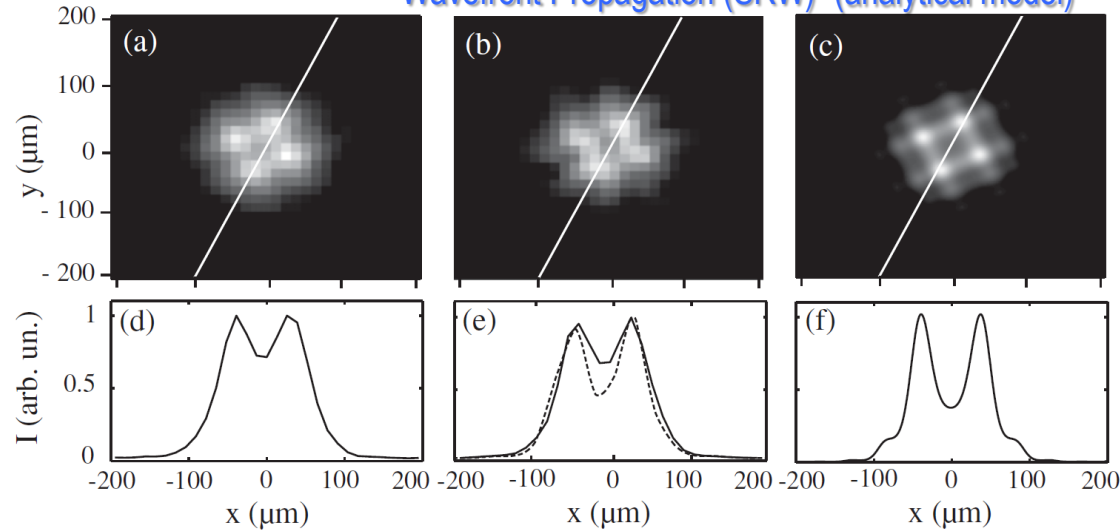
M.-E. Couprie
M. Idir
P. Mercier
R. Bachelard
M. Labat
T. Hara
et al.

At Fundamental Harmonic
Measured Simulated



Diffraction Pattern from One Rectangular Tilted Hole at 3rd Nonlinear Harmonic

Measured Simulated Simulated
SASE (Genesis) + Wavefront Propagation (SRW) Point Source (analytical model)



R. Bachelard et.al., PRL 106, 234801 (2011)

SRW Project Status (as of May 2013)

- “Synchrotron Radiation Workshop” (**SRW**) is electrodynamics / physical optics computer code for calculation of Synchrotron Radiation and simulation of Fully- and Partially-Coherent Radiation Wavefront Propagation
- SRW is written essentially in ANSI **C++**; **C API** is available (compiles as a 32- or 64-bit static or shared library for Windows, Linux, Mac OSX)
- Versions interfaced to **IGOR Pro** for Windows and Mac are available since **1997**:
<http://www.esrf.eu/Accelerators/Groups/InsertionDevices/Software/SRW>
- SRW for **Python** (2.7 and 3.2, 32- and 64-bit) versions are available for Windows and Linux since 2012
- **Parallel** versions of SRW for **Python** are available for partially-coherent wavefront propagation simulations (two test implementations: based on MPI / mpi4py, and using data exchange via files)
- SRW has been recently released to the **Open Source** under **BSD**-type license (the release procedure has been completed at BNL; permissions for the release were obtained from all Contributed Institutions and from US DOE):
<https://github.com/ochubar/SRW>
- Institutions and Individuals Contributed to SRW project:
 - **ESRF**: P.Elleaume, O.Chubar (O.C.), J.Chavanne, N.Canestrari (N.C.), M.S.del Rio
 - **SOLEIL**: O.C.
 - **BNL / PS**: O.C., N.C., R.Reininger (R.R.)
 - **E-XFEL GmbH**: L.Samoylova, G.Geloni, A.Buzmakov, I.Agapov
 - **DIAMOND LS Ltd.**: J.Sutter, D.Laundy, K.Sawhney
 - **ANL / APS**: R.R.
- On-going developments:
 - “thick” optical elements and library of mirror surfaces (under benchmarking);
 - X-ray diffraction by perfect crystals in Bragg and Laue geometries;
 - improving efficiency of 3D time (/frequency) dependent simulations for X-ray FEL and short-pulse THz–IR applications;
 - facilitating inter-operation with SHADOW ray-tracing code and other software



SRW Applications (Summary)

Accurate calculation of Electric Field and other characteristics of Synchrotron Radiation and simulation of Fully- and Partially-Coherent Wavefront Propagation within the framework of Physical Optics, implemented in SRW computer code, allows for a large variety of applications in such areas as:

- ✓ Development of New and Improvement of Existing Synchrotron Radiation Sources
 - ✓ Optimization of SR Beamlines for most efficient use of the properties of Sources and Optical Elements
 - ✓ Development of New types of Optical Elements for 3rd and 4th Generation Synchrotron Sources
 - ✓ Electron Beam, Insertion Device and Optical Element Characterization and Diagnostics
 - ✓ Simulation of User Experiments for most efficient use of Beam Time
- Potentially: use of SRW functions for Data Processing in Experiments in such areas as Imaging and Microscopy

Acknowledgements

- **J.-L. Laclare, P. Elleaume**
- A. Snigirev, I. Snigireva, J. Susini, M. Sanchez del Rio, J. Chavanne (ESRF)
- S. Molodtsov, L. Samoylova, G. Geloni, A. Buzmakov, I. Agapov, M. Yurkov, E. Saldin (European X-FEL / DESY)
- G. Materlik, K. Sawhney, J. Sutter, D. Laundry (DIAMOND)
- P. Dumas, M.-E. Couprie, P. Roy (SOLEIL)
- G. P. Williams (JLab)
- Y.-L. Mathis, P. Rieger (ANKA)
- V. Yashchuk, N. Artemiev, D. Robin, D. Shapiro (LBNL)
- R. Reininger, A. Khounsary, A. Zholents, Y. Shvydko (ANL)
- N. Smolyakov, S. Tomin (Kurchatov Inst.)
- J. Bahrtdt (BESSY)
- S. Dierker, Q. Shen, L. Berman, S. Krinsky, M. Idir, T. Shaftan, A. Fluerasu, L. Wiegart, K. Kaznatcheev, V. DeAndrade, Y. Chu, N. Canestrari, G. Bassi, A. Suvorov, P. Ilinski, V. Litvinenko (BNL)

SPARE SLIDES

Spontaneous Emission by Relativistic Electron in Free Space

Lienard-Wiechert Potentials for One Electron moving in Free Space:

$$\vec{A} = e \int_{-\infty}^{+\infty} \vec{\beta}_e R^{-1} \delta(\tau - t + R/c) d\tau, \quad \varphi = e \int_{-\infty}^{+\infty} R^{-1} \delta(\tau - t + R/c) d\tau \quad (\text{Gaussian CGS})$$

⇓

Electric Field in Frequency Domain (exact expressions!):

$$\vec{E}_\omega = \frac{ie\omega}{c} \int_{-\infty}^{+\infty} R^{-1} [\vec{\beta}_e - [1 + ic/(\omega R)] \vec{n}] \exp[i\omega(\tau + R/c)] d\tau \quad \text{I.M.Ternov used this approach in Far Field}$$

$$\vec{E}_\omega = \frac{e}{c} \int_{-\infty}^{+\infty} \frac{\vec{n} \times \left[(\vec{n} - \vec{\beta}_e) \times \dot{\vec{\beta}}_e \right] + cR^{-1} \gamma^{-2} (\vec{n} - \vec{\beta}_e)}{R \cdot (1 - \vec{n} \cdot \vec{\beta}_e)^2} \cdot \exp[i\omega(\tau + R/c)] d\tau \quad \text{J.D.Jackson}$$

The equivalence of the two expressions can be shown by integration by parts

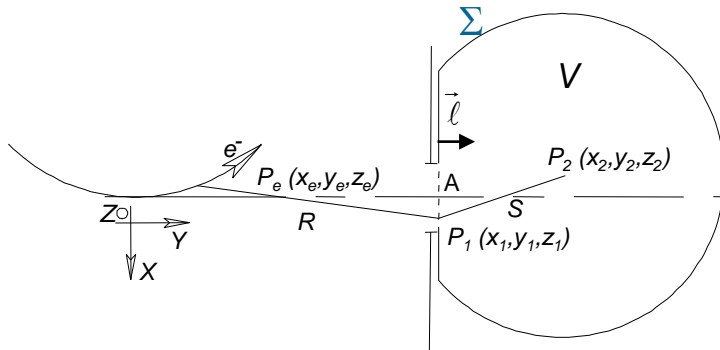
Phase Expansion (valid for the Near Field and in the Far Field Observation Conditions):

$$\omega \cdot (\tau + R/c) \approx \Phi_0 + \frac{\omega}{2} \left[\tau \gamma^{-2} + \int_0^\tau |\vec{\beta}_{e\perp}|^2 d\tilde{\tau} + \frac{|\vec{r}_\perp - \vec{r}_{e\perp}|^2}{c(z - c\tau)} \right]$$

$\vec{r}_{e\perp}, \vec{\beta}_{e\perp}$ are 2D vectors defining transverse coordinates and angles of electron trajectory
 \vec{r}_\perp is a 2D vector defining transverse coordinates of observation point
 z is longitudinal coordinate of observation point

Wavefront Propagation in the Case of Full Transverse Coherence

Kirchhoff Integral Theorem applied to Spontaneous Emission by One Electron



$$\vec{E}_{\omega 2\perp}(P_2) \approx \frac{k^2 e}{4\pi} \int_{-\infty}^{+\infty} d\tau \iint_A \frac{\vec{\beta}_{e\perp} - \vec{n}_\perp}{RS} \exp[ik(c\tau + R + S)] \cdot (\vec{\ell} \cdot \vec{n}_{P_e P_1} + \vec{\ell} \cdot \vec{n}_{P_1 P_2}) d\Sigma$$

Valid at large observation angles;
Is applicable to complicated cases of diffraction inside vacuum chamber

Huygens-Fresnel Principle

$$\vec{E}_{\omega 2\perp}(P_2) \approx \frac{k}{4\pi i} \iint_A \vec{E}_{\omega 1\perp}(P_1) \frac{\exp(ikS)}{S} (\vec{\ell} \cdot \vec{n} + \vec{\ell} \cdot \vec{n}_{P_1 P_2}) d\Sigma$$

Fourier Optics

Free Space:
(between parallel planes
perpendicular to optical axis)

$$\vec{E}_{\omega 2\perp}(x_2, y_2) \approx \frac{k}{2\pi i L} \iint \vec{E}_{\omega 1\perp}(x_1, y_1) \exp[ik[L^2 + (x_2 - x_1)^2 + (y_2 - y_1)^2]^{1/2}] dx_1 dy_1$$

Assumption of small angles

“Thin” Optical Element:

$$\vec{E}_{\omega 2\perp}(x, y) \approx \mathbf{T}(x, y, \omega) \vec{E}_{\omega 1\perp}(x, y)$$

“Thick” Optical Element:
(from transverse plane before
the element to a transverse
plane immediately after it)

$$\vec{E}_{\omega 2\perp}(x_2, y_2) \approx \mathbf{G}(x_2, y_2, \omega) \exp[ik\Lambda(x_2, y_2, k)] \vec{E}_{\omega 1\perp}(x_1(x_2, y_2), y_1(x_2, y_2))$$

E.g. from Stationary Phase method

Incoherent and Coherent Spontaneous Emission by Many Electrons

Electron Dynamics:

$$\begin{pmatrix} x_e \\ y_e \\ z_e \\ \beta_{xe} \\ \beta_{ye} \\ \delta\gamma_e \end{pmatrix} = \mathbf{A}(\tau) \begin{pmatrix} x_{e0} \\ y_{e0} \\ z_{e0} \\ x'_{e0} \\ y'_{e0} \\ \delta\gamma_{e0} \end{pmatrix} + \mathbf{B}(\tau) \quad \leftarrow \text{Initial Conditions}$$

Spectral Photon Flux per unit Surface emitted by the whole Electron Beam:

$$\frac{dN_{ph}}{dtdS(d\omega/\omega)} = \frac{c^2 \alpha I}{4\pi^2 e^3} \langle |\vec{E}_\omega|^2 \rangle$$

“Incoherent” SR

$$\langle |\vec{E}_\omega|^2 \rangle = \int \left| \vec{E}_{\omega 0}(\vec{r}; x_{e0}, y_{e0}, z_{e0}, x'_{e0}, y'_{e0}, \delta\gamma_{e0}) \right|^2 f(x_{e0}, y_{e0}, z_{e0}, x'_{e0}, y'_{e0}, \delta\gamma_{e0}) dx_{e0} dy_{e0} dz_{e0} dx'_{e0} dy'_{e0} d\delta\gamma_{e0} + (N_e - 1) \left| \int \vec{E}_{\omega 0}(\vec{r}; x_{e0}, y_{e0}, z_{e0}, x'_{e0}, y'_{e0}, \delta\gamma_{e0}) f(x_{e0}, y_{e0}, z_{e0}, x'_{e0}, y'_{e0}, \delta\gamma_{e0}) dx_{e0} dy_{e0} dz_{e0} dx'_{e0} dy'_{e0} d\delta\gamma_{e0} \right|^2$$

Coherent SR

Common Approximation for CSR: “Thin” Electron Beam: $\langle |\vec{E}_\omega|^2 \rangle_{CSR} \approx N_e \left| \int_{-\infty}^{\infty} \tilde{f}(z_{e0}) \exp(ikz_{e0}) dz_{e0} \right|^2 |\vec{E}_{\omega 1}|^2$

For Gaussian Longitudinal Bunch Profile: $\langle |\vec{E}_\omega|^2 \rangle_{CSR} \approx N_e \exp(-k^2 \sigma_b^2) |\vec{E}_{\omega 1}|^2$

If $f(x_{e0}, y_{e0}, z_{e0}, x'_{e0}, y'_{e0}, \delta\gamma_{e0})$ is Gaussian, 6-fold integration over electron phase space can be done analytically for the (Mutual) Intensity of Incoherent SR and for the Electric Field of CSR

Partially-Coherent SR Wavefront Propagation

Averaging of Propagated One-Electron Intensity

over Phase-Space Volume occupied by Electron Beam:

$$I_{\omega}(x, y) = \int I_{\omega 0}(x, y; x_{e0}, y_{e0}, z_{e0}, x'_{e0}, y'_{e0}, \delta\gamma_{e0}) f(x_{e0}, y_{e0}, z_{e0}, x'_{e0}, y'_{e0}, \delta\gamma_{e0}) dx_{e0} dy_{e0} dz_{e0} dx'_{e0} dy'_{e0} d\delta\gamma_{e0}$$

Convolution is valid in simple cases:

- projection geometry;
- focusing by a thin lens;
- diffraction on one slit (/pinhole);
- ...

$$I_{\omega}(x, y) \approx \int_{-\infty-\infty}^{+\infty+\infty} \int \tilde{I}_{\omega 0}(x - \tilde{x}_e, y - \tilde{y}_e) \tilde{f}(\tilde{x}_e, \tilde{y}_e) d\tilde{x}_e d\tilde{y}_e$$

OR:

Propagation of Mutual Intensity

Initial Mutual Intensity:

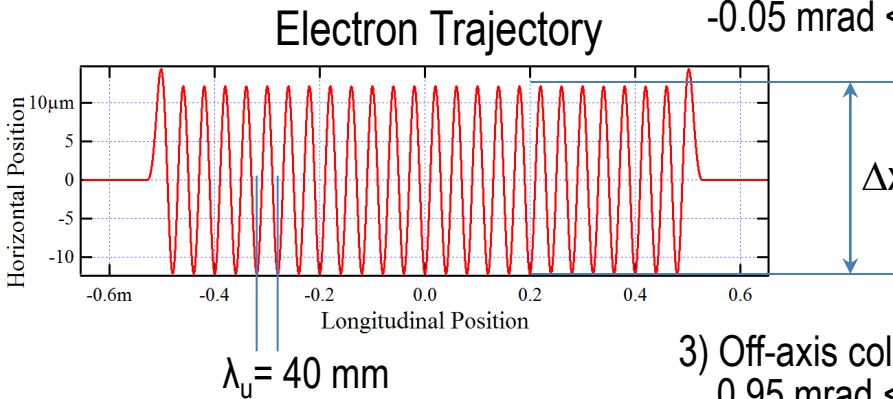
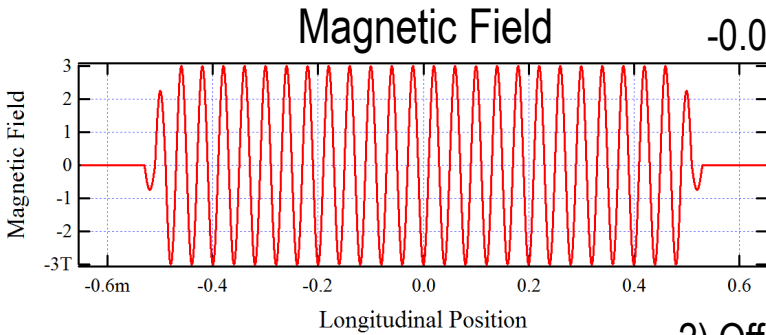
$$M_{\omega}(x, y; \tilde{x}, \tilde{y}) = \int \vec{E}_{\omega 0 \perp}(x, y; x_{e0}, y_{e0}, z_{e0}, x'_{e0}, y'_{e0}, \delta\gamma_{e0}) \vec{E}_{\omega 0 \perp}^*(\tilde{x}, \tilde{y}; x_{e0}, y_{e0}, z_{e0}, x'_{e0}, y'_{e0}, \delta\gamma_{e0}) \\ \times f(x_{e0}, y_{e0}, z_{e0}, x'_{e0}, y'_{e0}, \delta\gamma_{e0}) dx_{e0} dy_{e0} dz_{e0} dx'_{e0} dy'_{e0} d\delta\gamma_{e0}$$

Wigner Distribution (or mathematical Brightness):

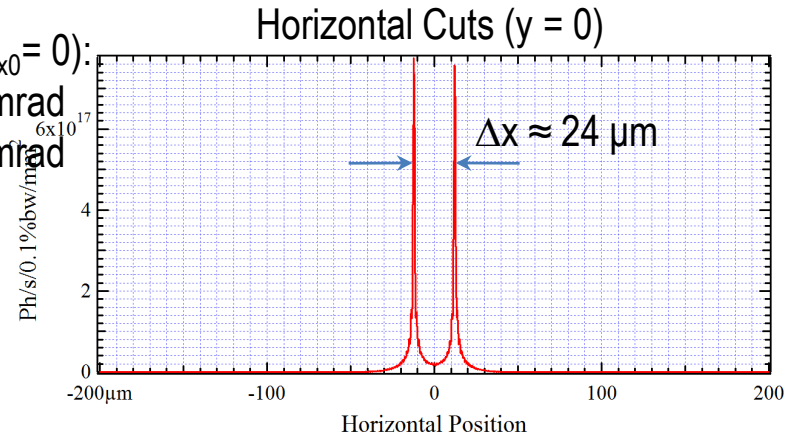
$$B_{\omega}(x, y; \theta_x, \theta_y) = \frac{1}{2\pi} \int_{-\infty-\infty}^{+\infty+\infty} \int M_{\omega}(x, y; \tilde{x}, \tilde{y}) \exp[ik(\theta_x \tilde{x} + \theta_y \tilde{y})] d\tilde{x} d\tilde{y}$$

Intensity Distributions of Focused Wiggler Radiation (1 : 1)

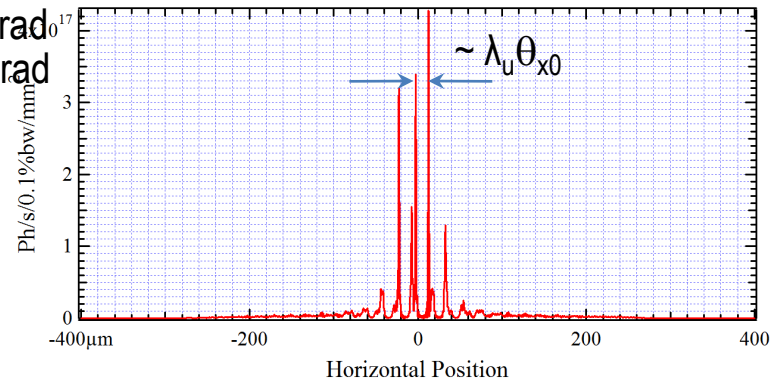
Wavefront Propagation Calculations for "Filament" Electron Beam



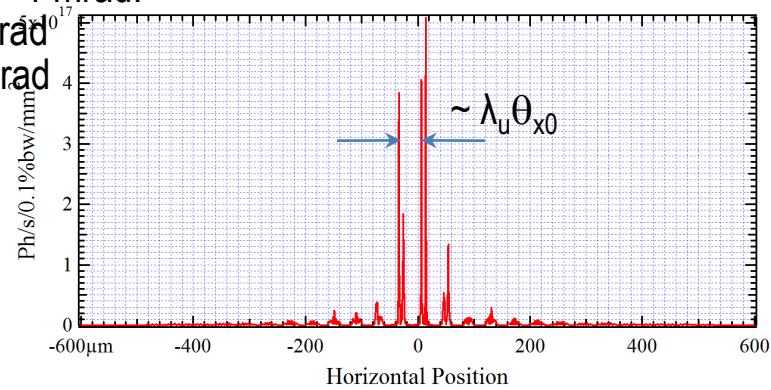
- 1) On-axis collection (at $\theta_{x0} = 0$):
 $-0.05 \text{ mrad} < \theta_x < 0.05 \text{ mrad}$
 $-0.05 \text{ mrad} < \theta_y < 0.05 \text{ mrad}$



- 2) Off-axis collection at $\theta_{x0} = 0.5 \text{ mrad}$:
 $0.45 \text{ mrad} < \theta_x < 0.55 \text{ mrad}$
 $-0.05 \text{ mrad} < \theta_y < 0.05 \text{ mrad}$



- 3) Off-axis collection at $\theta_{x0} = 1 \text{ mrad}$:
 $0.95 \text{ mrad} < \theta_x < 1.05 \text{ mrad}$
 $-0.05 \text{ mrad} < \theta_y < 0.05 \text{ mrad}$



E-beam: $E = 3 \text{ GeV}$, $I = 0.5 \text{ A}$
 SCW40: $\lambda_u = 40 \text{ mm}$, $B_{\text{max}} = 3 \text{ T}$, $L = 1 \text{ m}$
 Photon Energy used in calc.: $E_{\text{ph}} = 10 \text{ keV}$

Features of Some Existing Free Computer Codes

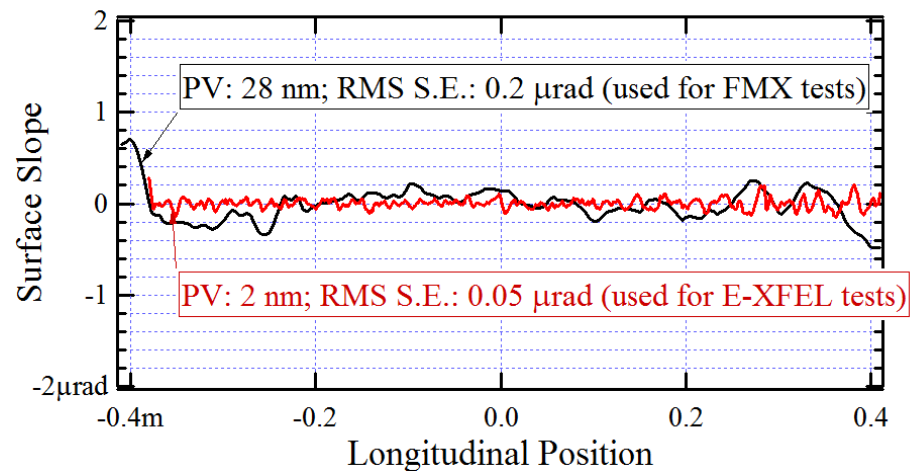
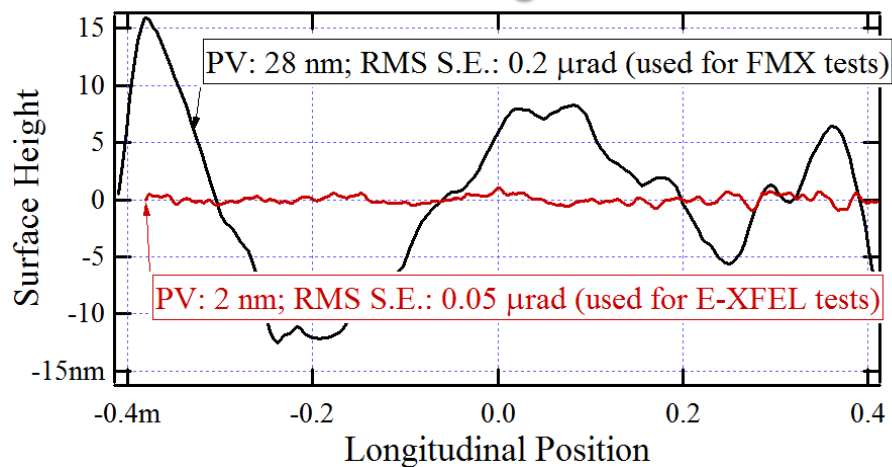
Features \ Codes	SPECTRA	WAVE	GENESIS	SHADOW	RAY	PHASE	SRW
Source Simulation	Y	Y	Y	Y(?)	N(?)	N(?)	Y
Gaussian Beams	Y	Y	Y	Y	Y	Y(?)	Y
Spontaneous SR	Y	Y	N(?)	Y (BM?)	N(?)	N	Y
Single-Electron	Y	Y	N(?)	N	N(?)	N	Y
Incoherent "Multi-Electron"	Y	Y(?)	N(?)	Y (BM?)	N(?)	N	Y
CSR	Y(?)	Y(?)	N(?)	N	N(?)	N	Y
SASE	N	N	Y	N	N(?)	N	N(?)
Geometrical Ray-Tracing	N	N	N	Y	Y	N	N
Wavefront Propagation	N(?)	N	N(?)	N	N(?)	Y	Y
Fully-Coherent Beams						Y	Y
Partially-Coherent Beams						N(?)	Y
Time-/Frequency-Dependent						Y(?)	Y
Optical Elements	N	N	N	Y	Y	Y	Y
Grazing-Incidence Mirrors				Y	Y	Y	Y(?)
Refractive Optics				Y	Y	Y	Y
Diffractive Optics				N	Y	Y(?)	Y
Gratings				Y(?)	Y	Y	N(?)
Crystals				Y	Y	N(?)	N(?)
Framework	Y	Y	Y	Y	Y	Y	Y
Scripting Environment	N(?)	N(?)	N(?)	Y(?)	N(?)	N(?)	Y
File Input-Output	Y	Y	Y	Y	Y	Y	Y(?)
GUI	Y(?)	Y	N(?)	Y(?)	Y	Y	Y(?)
API	N(?)	N(?)	N(?)	N	N(?)	N(?)	Y
Cross-Platform	Y(?)	Y(?)	Y	Y	Y	Y	Y
Open Source	N(?)	N(?)	Y	Y	N(?)	N	Y
Development Effort (man-years to date, full time)	?	?	~4(?)	~5(?)	?	~3(?)	~4

Height Profiles and Slope Errors of Some Mirror

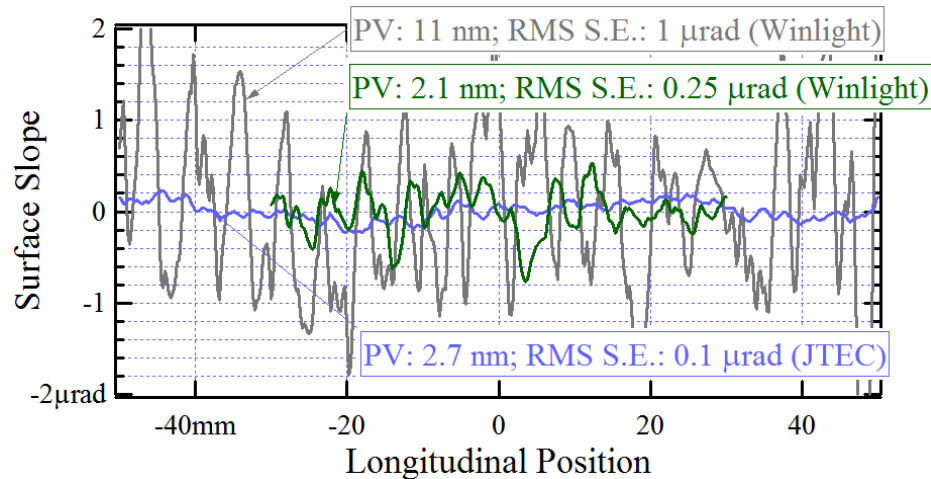
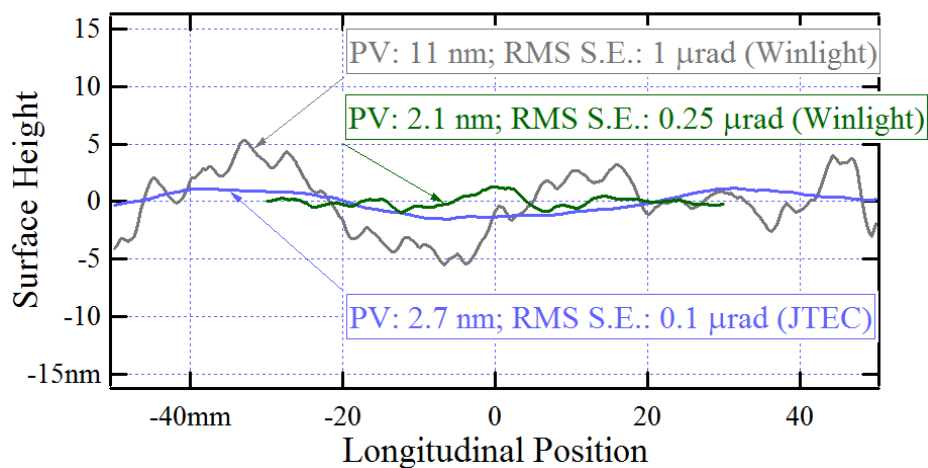
Height Profiles

Slope Errors

Long Mirror Considered for FMX BL Tests

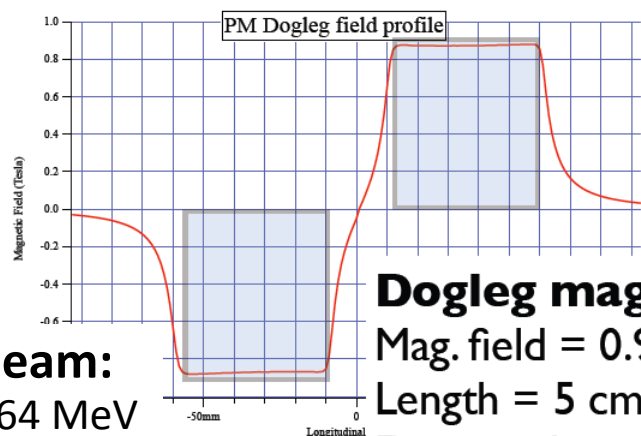


Short Mirrors Considered for SRX BL Tests



Data from M. Idir, R. Sweet, V. DeAndrade (BNL), L. Samoylova (E-XFEL)

Non-Destructive Single-Shot E-Beam Emittance Measurement in ERL / FEL Injectors Using Interfering Edge Radiation



e-beam:
 $E = 64 \text{ MeV}$
 $dE/E = 2e-4$
 $Q = 500 \text{ pC}$
 $\epsilon_N \approx 2 \mu\text{m}$

Doleg magnets:
 Mag. field = 0.9 T
 Length = 5 cm
 Distance between magnets = 2 cm

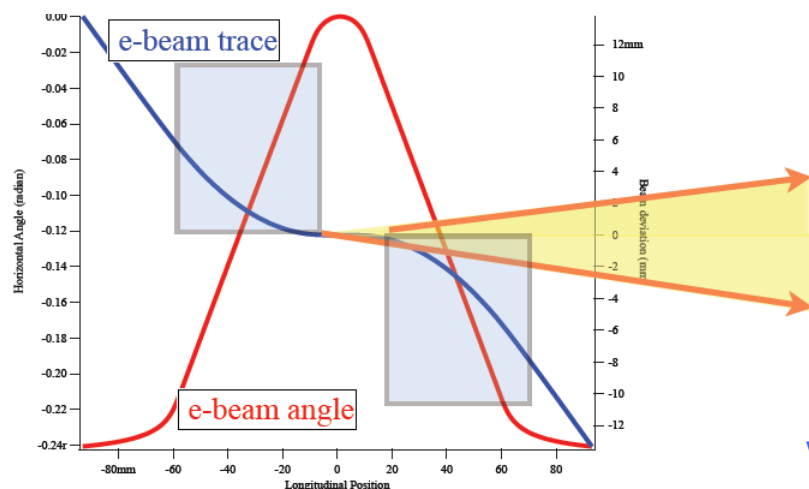
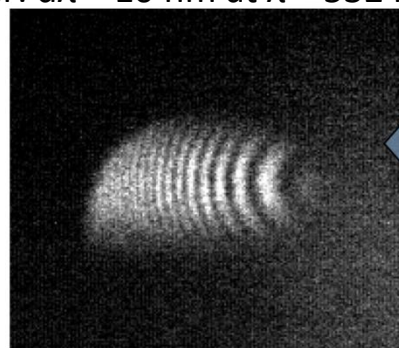
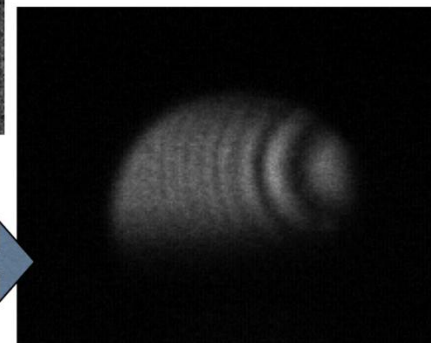
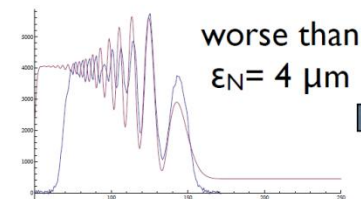
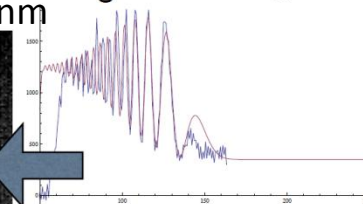


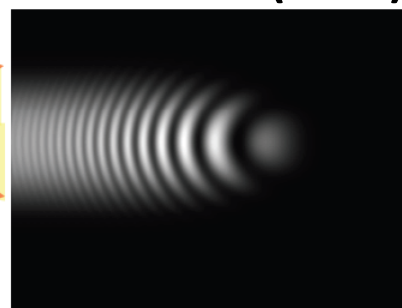
Image of PI camera, filter: $d\lambda = 10 \text{ nm}$ at $\lambda = 532 \text{ nm}$



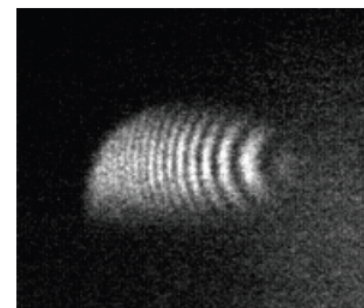
good fit to $\epsilon_N = 1.9 \mu\text{m}$



Simulation (SRW)



Measurement



V. Yakimenko, M. Fedurin (ATF, BNL, June 2012)



U.S. DEPARTMENT OF
ENERGY

Method: O.C., Rev. Sci. Instrum., 1995, vol.66 (2), p.1872 (SRI-1994); "Siberia-1", Kurchatov Institute, Moscow

BROOKHAVEN
 NATIONAL LABORATORY
 BROOKHAVEN SCIENCE ASSOCIATES